



NATIONAL CENTRE OF COMPETENCE IN RESEARCH

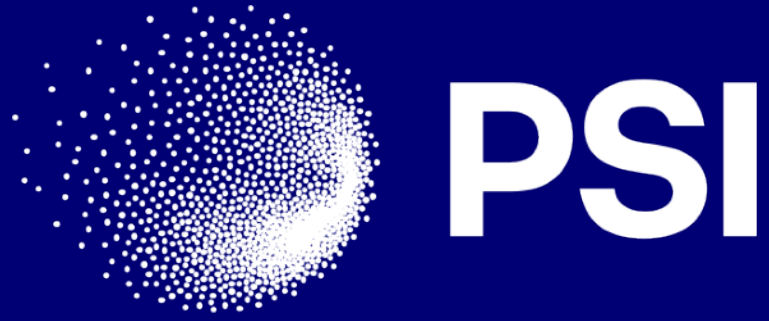


First-principles calculation of Hubbard parameter using linear-response theory

Iurii Timrov

Paul Scherrer Institute, Switzerland

ICTP-MARVEL College, 5 June 2026



NATIONAL CENTRE OF COMPETENCE IN RESEARCH



First-principles calculation of Hubbard parameter using linear-response theory

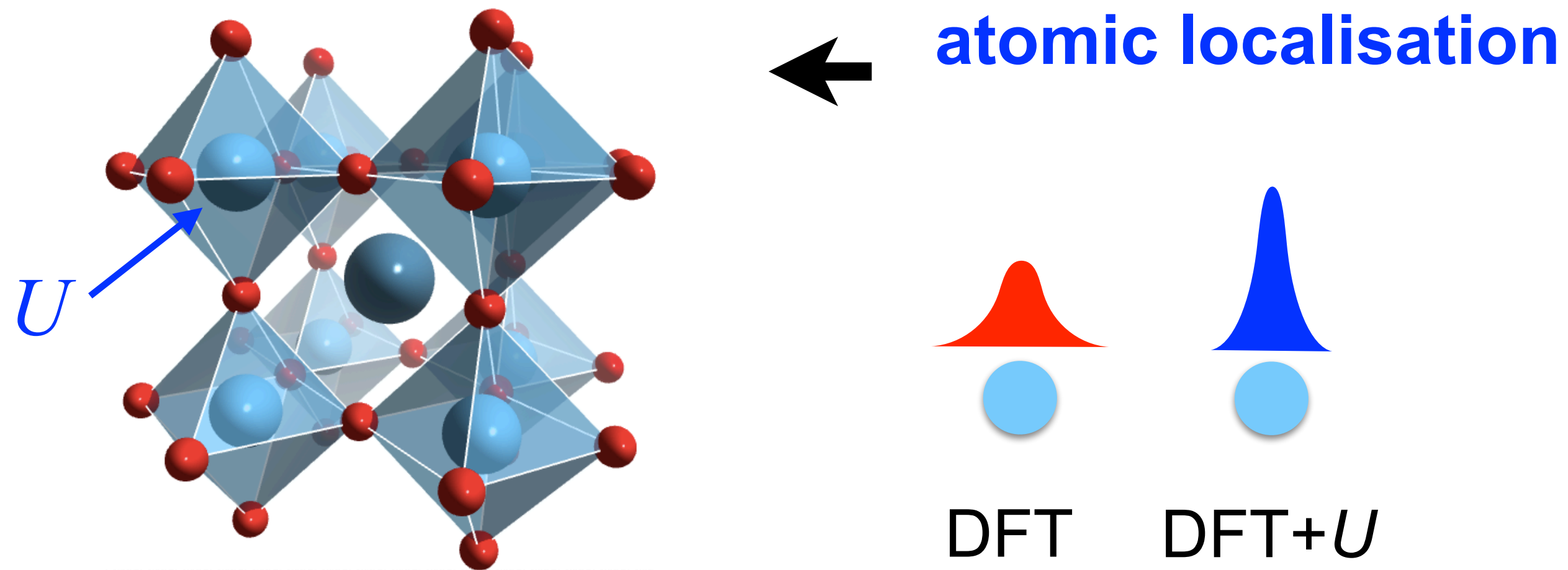
Iurii Timrov

Paul Scherrer Institute, Switzerland

ICTP-MARVEL College, 5 June 2026

DFT+U(+V)

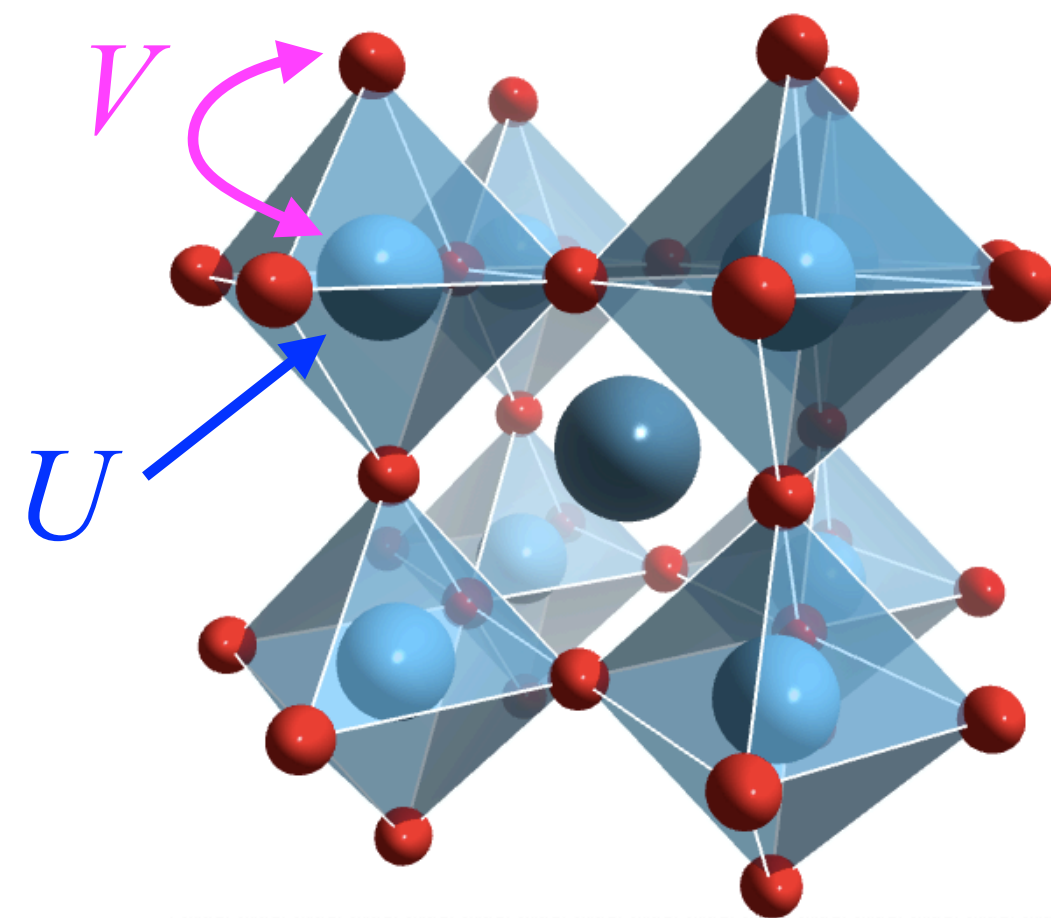
DFT+U : $E = E_{\text{DFT}} + \frac{1}{2} \sum_{I,\sigma} U^I \text{Tr} [(\mathbf{1} - \mathbf{n}^{I\sigma}) \mathbf{n}^{I\sigma}]$ $(\mathbf{n}^{I\sigma})_{m_1 m_2} = \sum_i f_i \langle \psi_{i\sigma} | \varphi_{m_2}^I \rangle \langle \varphi_{m_1}^I | \psi_{i\sigma} \rangle$



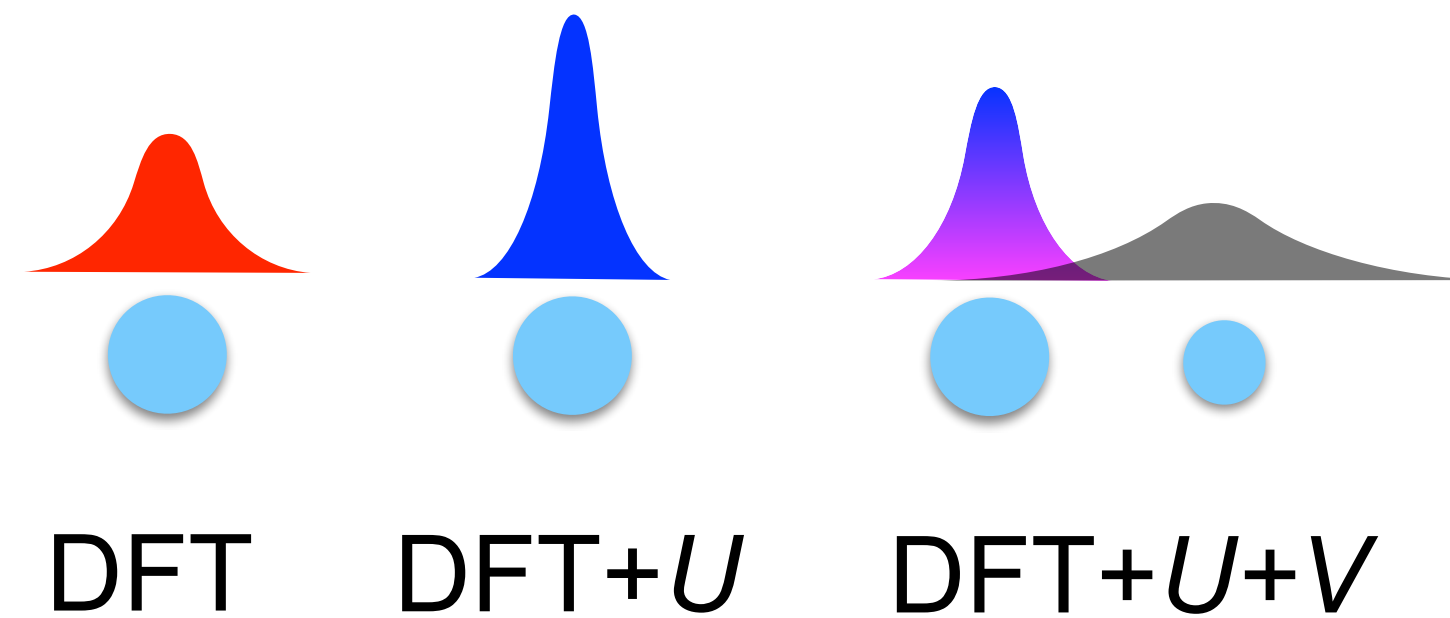
DFT+U(+V)

DFT+U : $E = E_{\text{DFT}} + \frac{1}{2} \sum_{I,\sigma} U^I \text{Tr} [(\mathbf{1} - \mathbf{n}^{I\sigma}) \mathbf{n}^{I\sigma}]$ $(\mathbf{n}^{I\sigma})_{m_1 m_2} = \sum_i f_i \langle \psi_{i\sigma} | \varphi_{m_2}^I \rangle \langle \varphi_{m_1}^I | \psi_{i\sigma} \rangle$

DFT+U+V : $E = E_{\text{DFT}} + \frac{1}{2} \sum_{I,\sigma} U^I \text{Tr} [(\mathbf{1} - \mathbf{n}^{I\sigma}) \mathbf{n}^{I\sigma}] - \frac{1}{2} \sum_{I,J,\sigma} V^{IJ} \text{Tr} [\mathbf{n}^{IJ\sigma} \mathbf{n}^{JI\sigma}]$



← **atomic localisation & inter-atomic hybridisations**



Hubbard parameters and Hubbard projectors



Hubbard parameters and Hubbard projectors

$$E = E_{\text{DFT}} + \frac{1}{2} \sum_{I,\sigma} U^I \text{Tr} [(1 - \mathbf{n}^{I\sigma}) \mathbf{n}^{I\sigma}] - \frac{1}{2} \sum_{I,J,\sigma} V^{IJ} \text{Tr} [\mathbf{n}^{IJ\sigma} \mathbf{n}^{JI\sigma}]$$

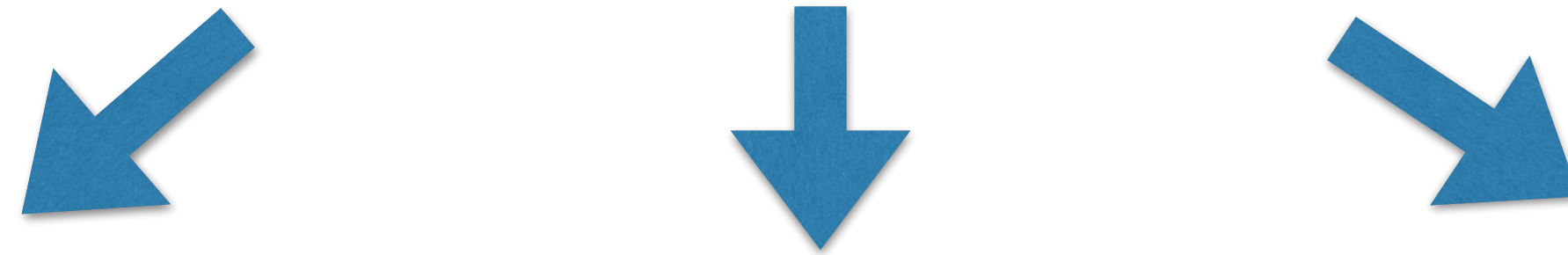
**Hubbard
parameters**

**Hubbard
projectors**

$$(\mathbf{n}^{IJ\sigma})_{m_1 m_2} = \sum_i f_i \langle \psi_{i\sigma} | \varphi_{m_2}^J \rangle \langle \varphi_{m_1}^I | \psi_{i\sigma} \rangle$$

How to determine Hubbard parameters?

Strategies



Fitting to experiments

magnetic moments

band gaps

oxidation enthalpies

Fitting to other advanced methods

HSE06

PBE0

GW

First-principles calculations

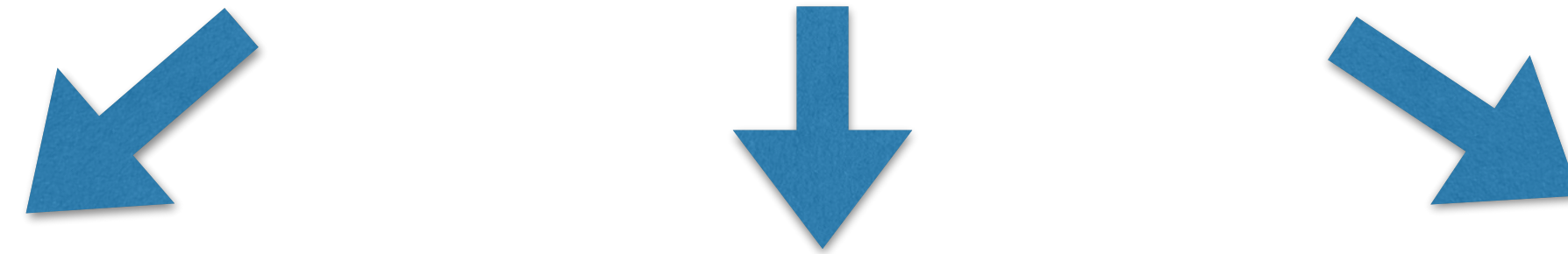
Linear response theory (LRT)

constrained RPA (cRPA)

Hartree-Fock (ACBN0)

How to determine Hubbard parameters?

Strategies



Fitting to experiments

magnetic moments

band gaps

oxidation enthalpies

Fitting to other advanced methods

HSE06

PBE0

GW

First-principles calculations

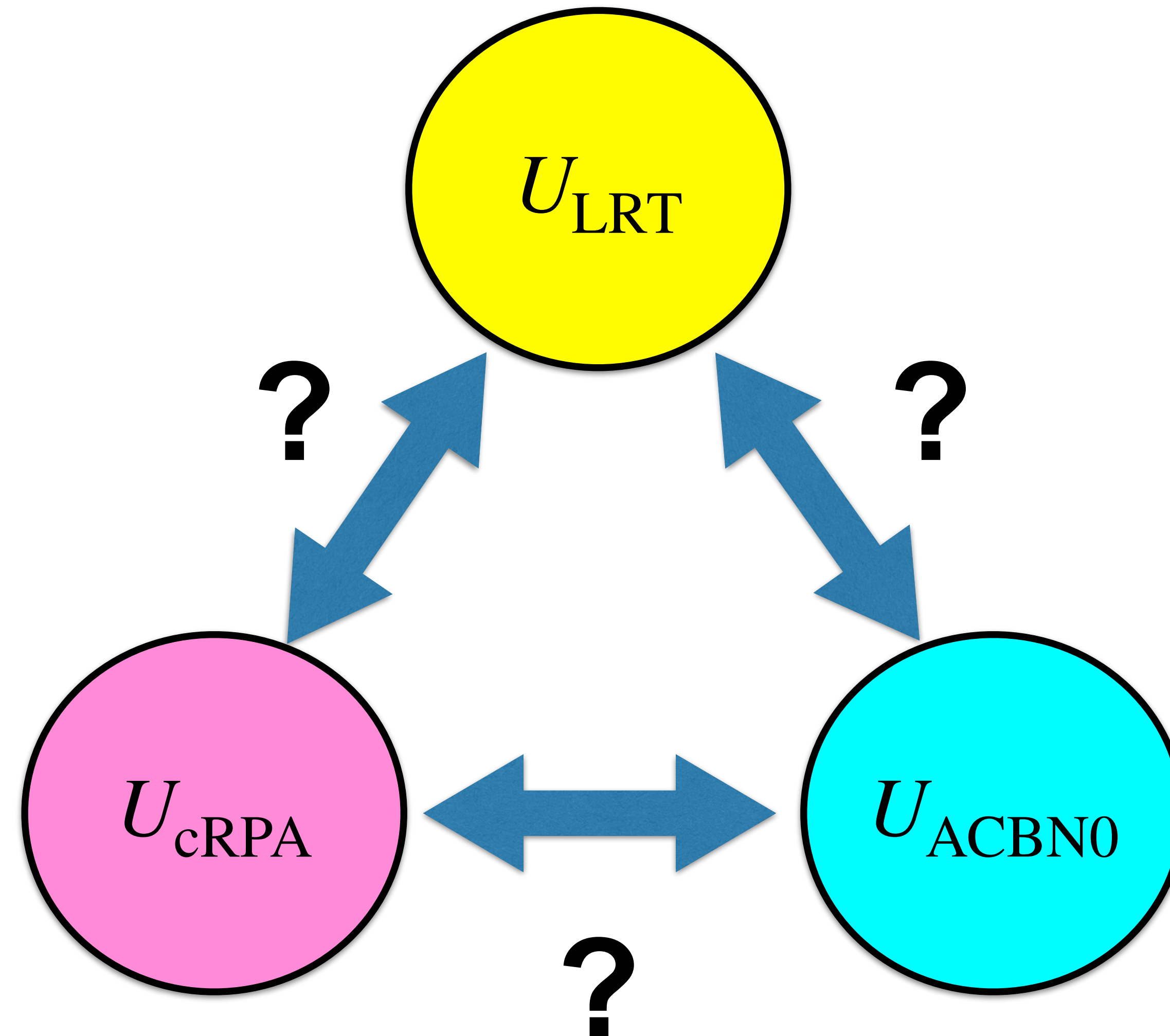
Linear response theory (LRT)

constrained RPA (cRPA)

Hartree-Fock (ACBN0)

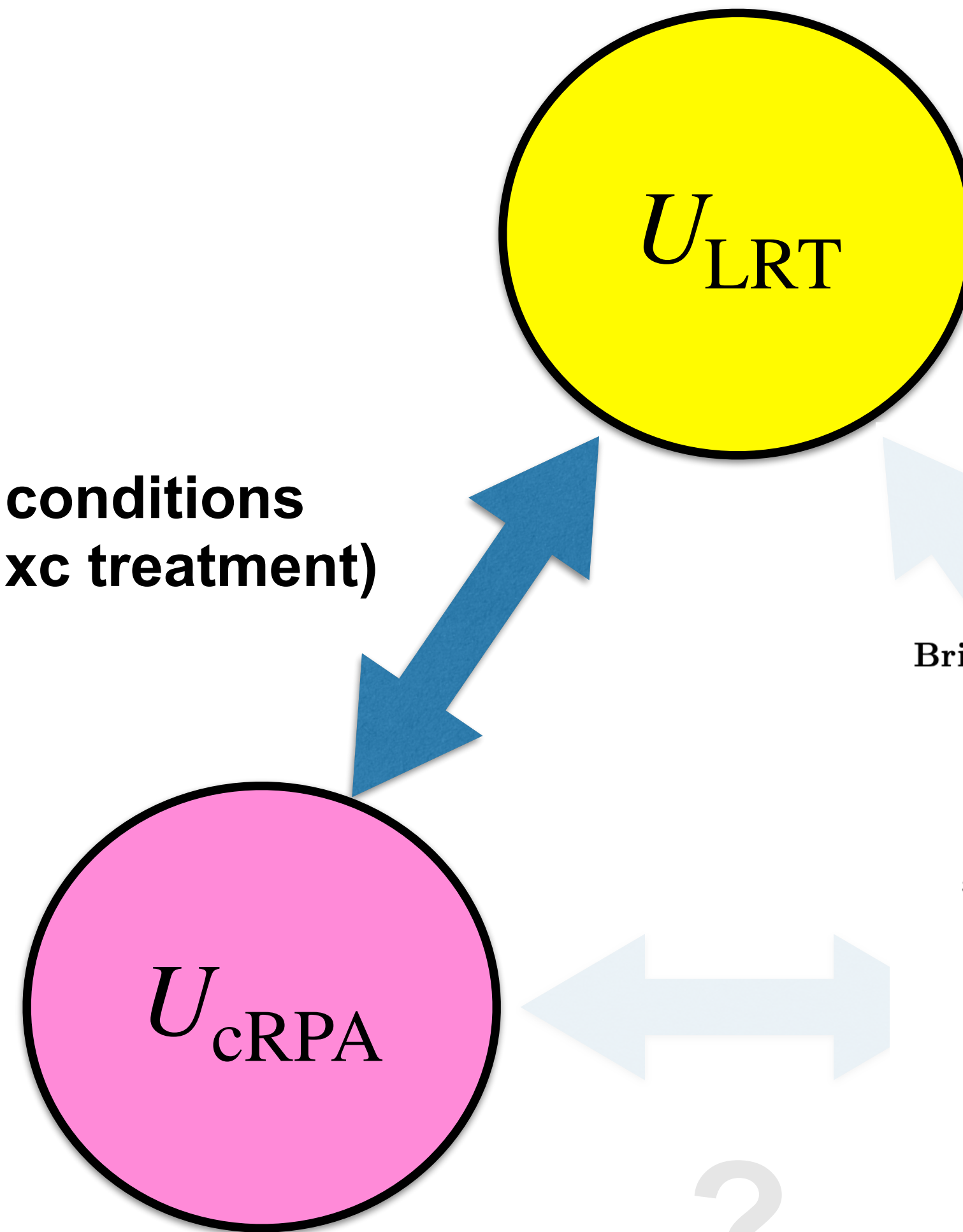
machine learning

Are the U values the same from different methods?



Are the U values the same from different methods?

Yes, under certain conditions
(coarse graining and xc treatment)



accepted to PRL

Bridging constrained random-phase approximation and linear response theory for computing Hubbard parameters

Alberto Carta,^{1,2,*} Iurii Timrov,^{2,†} Sophie Beck,³ and Claude Ederer^{1,‡}

¹Materials Theory, ETH Zürich, Wolfgang-Pauli-Strasse 27, 8093 Zürich, Switzerland

²PSI Center for Scientific Computing, Theory, and Data,
Paul Scherrer Institute, 5232 Villigen PSI, Switzerland

³Center for Computational Quantum Physics, Flatiron Institute, 162 5th Avenue, New York, NY 10010, USA

(Dated: December 24, 2025)

The predictive accuracy of popular extensions to density-functional theory (DFT) such as DFT+ U and DFT plus dynamical mean-field theory (DFT+DMFT) hinges on using realistic values for the screened Coulomb interaction U . Here, we present a systematic comparison of the two most widely used approaches to compute this parameter, *i.e.* linear response theory (LRT) and the constrained random-phase approximation (cRPA), using a unified framework based on the use of maximally localized Wannier functions. We show that the U in LRT and cRPA can differ as much as 30%. We demonstrate that this discrepancy arises from two main differences: neglecting the response of the exchange-correlation potential in cRPA and additional excitation channels in LRT. By taking these differences into account, we can achieve near perfect agreement between the two techniques. Moreover, we show that in cases with strong hybridization between interacting and screening subspaces, the application of cRPA becomes ambiguous and can lead to unrealistically small U values, while LRT remains well-behaved. Our work formally connects both methods, sheds light on their strengths and limitations, and emphasizes the importance of using a consistent set of Wannier orbitals to ensure transferability of U values between different implementations.

Are the U values the same from different methods?

npj | computational materials (in press)

Explore content ▾ About the journal ▾ Publish with us ▾

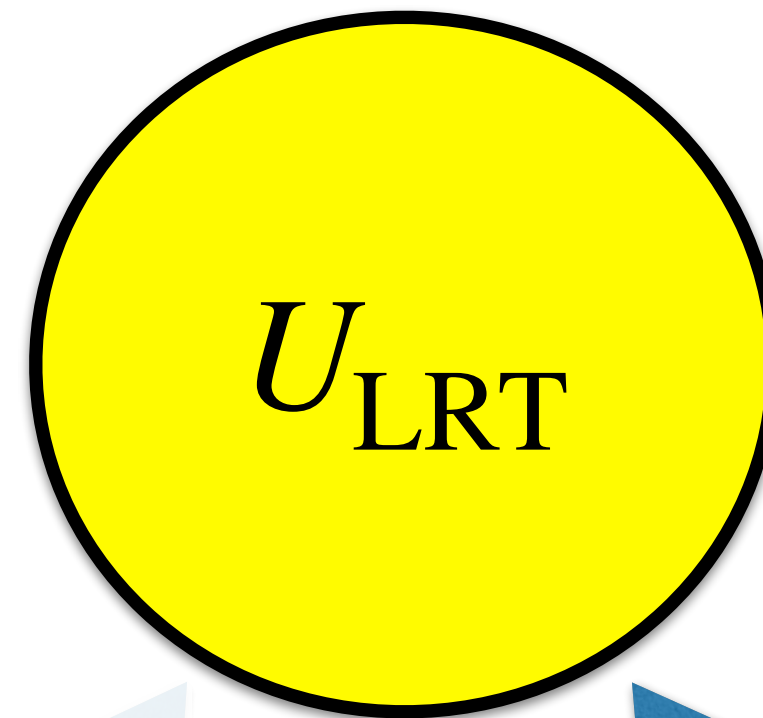
[nature](#) > [npj computational materials](#) > [articles](#) > [article](#)

Article | [Open access](#) | Published: 16 May 2026

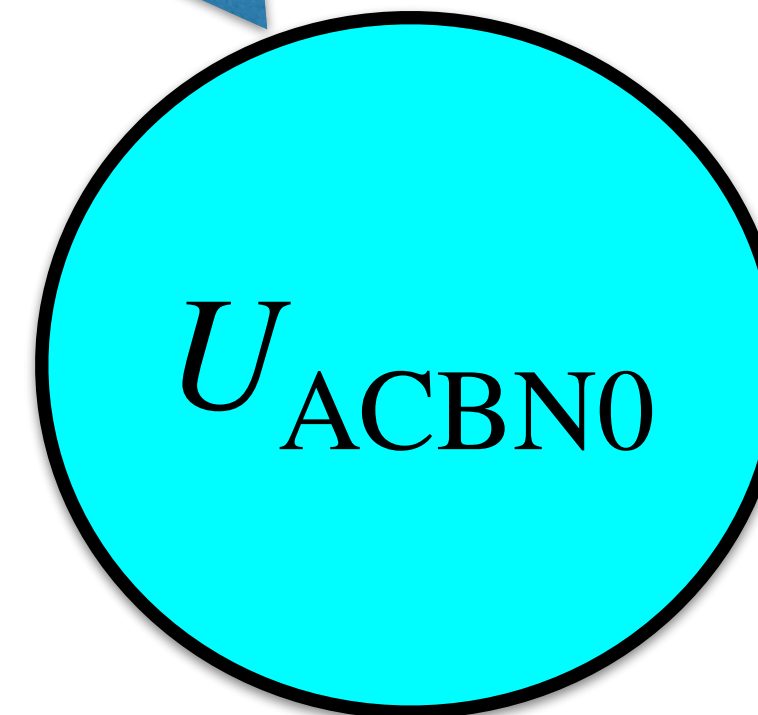
Comparing Hubbard parameters from linear-response theory and a Hartree-Fock-based approach

[Wooil Yang](#), [Iurii Timrov](#) , [Francesco Aquilante](#) & [Young-Woo Son](#) 

[npj Computational Materials](#) (2026) | [Cite this article](#)



Similar for partially filled states
and
Very different for nearly empty
or fully filled states



Hubbard parameters are not universal

Computed Hubbard parameters depend on:

- **Type of Hubbard projector functions** (e.g. atomic, Wannier, etc.)

$$(\mathbf{n}^{I\sigma})_{m_1 m_2} = \sum_i f_i \langle \psi_{i\sigma} | \varphi_{m_2}^I \rangle \langle \varphi_{m_1}^I | \psi_{i\sigma} \rangle$$

Hubbard parameters are not universal

Computed Hubbard parameters depend on:

- **Type of Hubbard projector functions** (e.g. atomic, Wannier, etc.)

$$(\mathbf{n}^{I\sigma})_{m_1 m_2} = \sum_i f_i \langle \psi_{i\sigma} | \varphi_{m_2}^I \rangle \langle \varphi_{m_1}^I | \psi_{i\sigma} \rangle$$

- **Pseudopotential and the oxidation state**

Hubbard parameters are not universal

Computed Hubbard parameters depend on:

- **Type of Hubbard projector functions** (e.g. atomic, Wannier, etc.)

$$(\mathbf{n}^{I\sigma})_{m_1 m_2} = \sum_i f_i \langle \psi_{i\sigma} | \varphi_{m_2}^I \rangle \langle \varphi_{m_1}^I | \psi_{i\sigma} \rangle$$

- **Pseudopotential and the oxidation state**
- **Exchange-correlation functional** (e.g. LDA, GGA, etc.)

Hubbard parameters are not universal

Computed Hubbard parameters depend on:

- **Type of Hubbard projector functions** (e.g. atomic, Wannier, etc.)

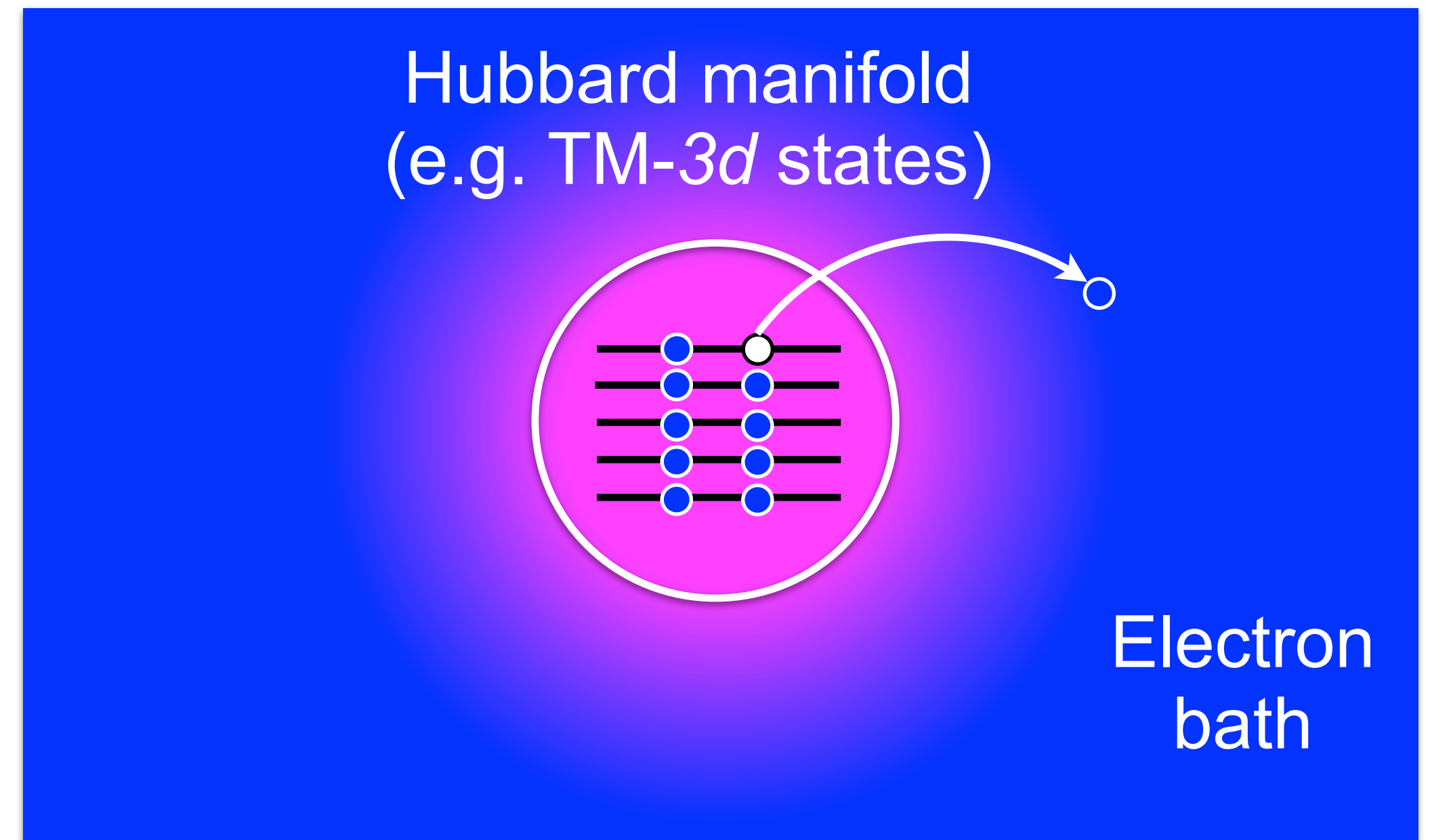
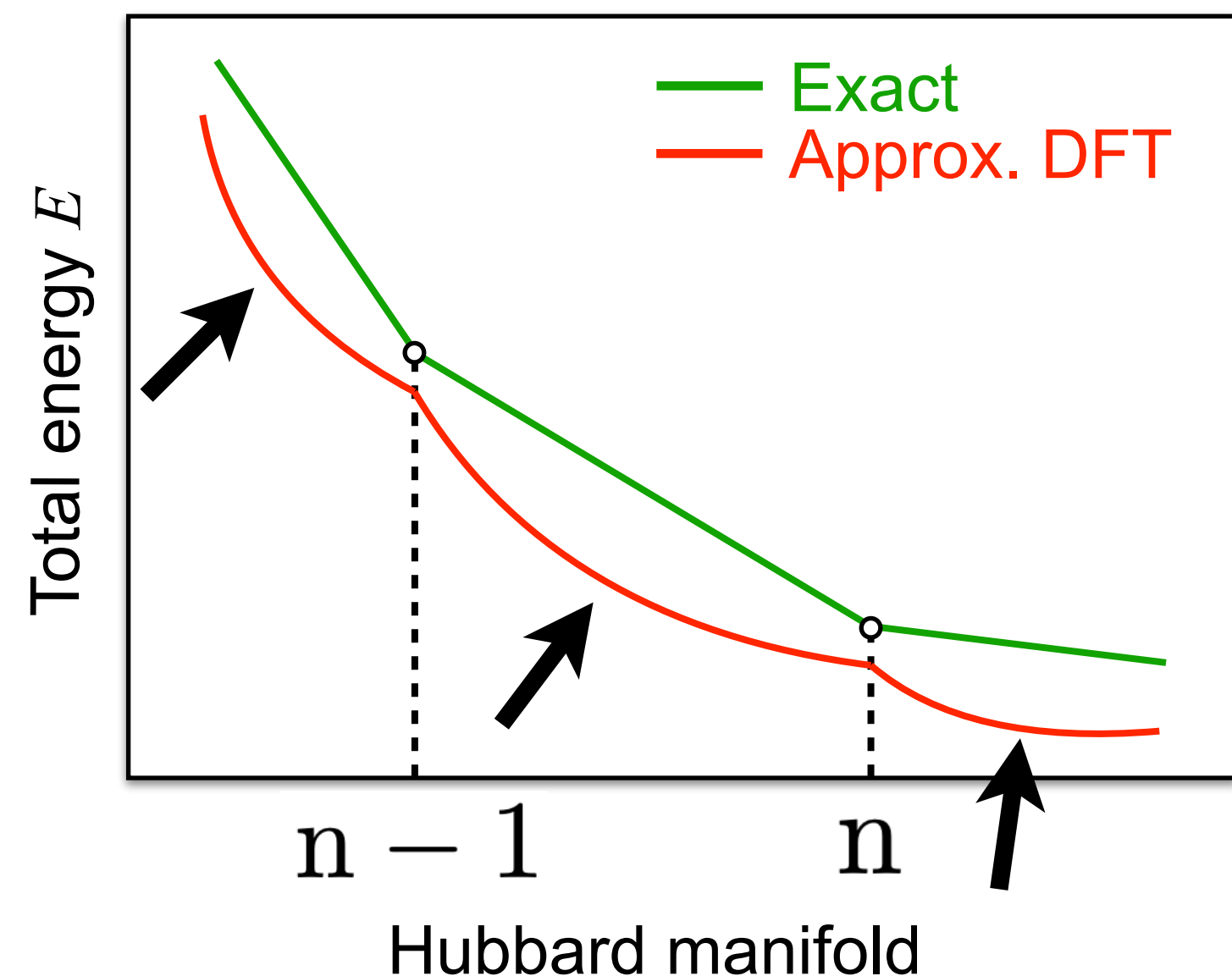
$$(\mathbf{n}^{I\sigma})_{m_1 m_2} = \sum_i f_i \langle \psi_{i\sigma} | \varphi_{m_2}^I \rangle \langle \varphi_{m_1}^I | \psi_{i\sigma} \rangle$$

- **Pseudopotential and the oxidation state**
- **Exchange-correlation functional** (e.g. LDA, GGA, etc.)
- **Self-consistency** (i.e. either “one-shot” or self-consistent)

Hubbard U from linear response theory (LRT)

$$E = E_{\text{DFT}} + \frac{1}{2} U \text{Tr} [(\mathbf{1} - \mathbf{n}) \mathbf{n}]$$

Heuristic statement: Energy changes in a linear fashion when moving electrons from the Hubbard manifold to the rest of the system.



Definition of Hubbard U :

$$\frac{d^2 E}{dn^2} = 0 \quad \Rightarrow \quad U = \frac{d^2 E_{\text{DFT}}}{dn^2}$$

Linear response theory (LRT)

Legendre transformation and minimization of the total energy w.r.t spin-charge density ρ_σ :

$$E(\{\lambda^I\}) = \min_{\rho_\sigma} \left\{ E_{\text{DFT}}[\rho_\sigma] + \sum_I \lambda^I n^I \right\}$$

Linear response theory (LRT)

Legendre transformation and minimization of the total energy w.r.t spin-charge density ρ_σ :

$$E(\{\lambda^I\}) = \min_{\rho_\sigma} \left\{ E_{\text{DFT}}[\rho_\sigma] + \sum_I \lambda^I n^I \right\} \quad \rightarrow \quad \bar{E}(\{n^I\}) = E(\{\lambda^I\}) - \sum_I \lambda^I n^I$$

Linear response theory (LRT)

Legendre transformation and minimization of the total energy w.r.t spin-charge density ρ_σ :

$$E(\{\lambda^I\}) = \min_{\rho_\sigma} \left\{ E_{\text{DFT}}[\rho_\sigma] + \sum_I \lambda^I n^I \right\} \quad \rightarrow \quad \bar{E}(\{n^I\}) = E(\{\lambda^I\}) - \sum_I \lambda^I n^I$$

Compute the 1st and 2nd derivatives:

$$\frac{d\bar{E}}{dn^I} = -\lambda^I \qquad \frac{d^2\bar{E}}{d(n^I)^2} = -\frac{d\lambda^I}{dn^I} = -(\chi^{-1})_{II}$$

Linear response theory (LRT)

Legendre transformation and minimization of the total energy w.r.t spin-charge density ρ_σ :

$$E(\{\lambda^I\}) = \min_{\rho_\sigma} \left\{ E_{\text{DFT}}[\rho_\sigma] + \sum_I \lambda^I n^I \right\} \quad \rightarrow \quad \bar{E}(\{n^I\}) = E(\{\lambda^I\}) - \sum_I \lambda^I n^I$$

Compute the 1st and 2nd derivatives:

$$\frac{d\bar{E}}{dn^I} = -\lambda^I \qquad \frac{d^2\bar{E}}{d(n^I)^2} = -\frac{d\lambda^I}{dn^I} = -(\chi^{-1})_{II}$$

The Hubbard U parameter is defined as:

$$\boxed{U^I} = [- (\chi^{-1})_{II}] - [- (\chi_0^{-1})_{II}] = \boxed{(\chi_0^{-1} - \chi^{-1})_{II}}$$

← not related to e-e interactions

Linear response theory (LRT)

Legendre transformation and minimization of the total energy w.r.t spin-charge density ρ_σ :

$$E(\{\lambda^I\}) = \min_{\rho_\sigma} \left\{ E_{\text{DFT}}[\rho_\sigma] + \sum_I \lambda^I n^I \right\} \quad \rightarrow \quad \bar{E}(\{n^I\}) = E(\{\lambda^I\}) - \sum_I \lambda^I n^I$$

Compute the 1st and 2nd derivatives:

$$\frac{d\bar{E}}{dn^I} = -\lambda^I \qquad \frac{d^2\bar{E}}{d(n^I)^2} = -\frac{d\lambda^I}{dn^I} = -(\chi^{-1})_{II}$$

The Hubbard U parameter is defined as:

Dyson equation:

$$\boxed{U^I} = [- (\chi^{-1})_{II}] - [- (\chi_0^{-1})_{II}] = \boxed{(\chi_0^{-1} - \chi^{-1})_{II}} \quad \leftrightarrow \quad \boxed{\chi = \chi_0 + \chi_0 U \chi}$$

not related to e-e interactions

LRT using supercells and finite differences

Modified Kohn-Sham equations:

$$\left(\hat{H}_\sigma + \lambda^J \hat{V}_{\text{pert}}^J \right) |\psi_{v\mathbf{k}\sigma}\rangle = \varepsilon_{v\mathbf{k}\sigma} |\psi_{v\mathbf{k}\sigma}\rangle$$

Perturbing potential:

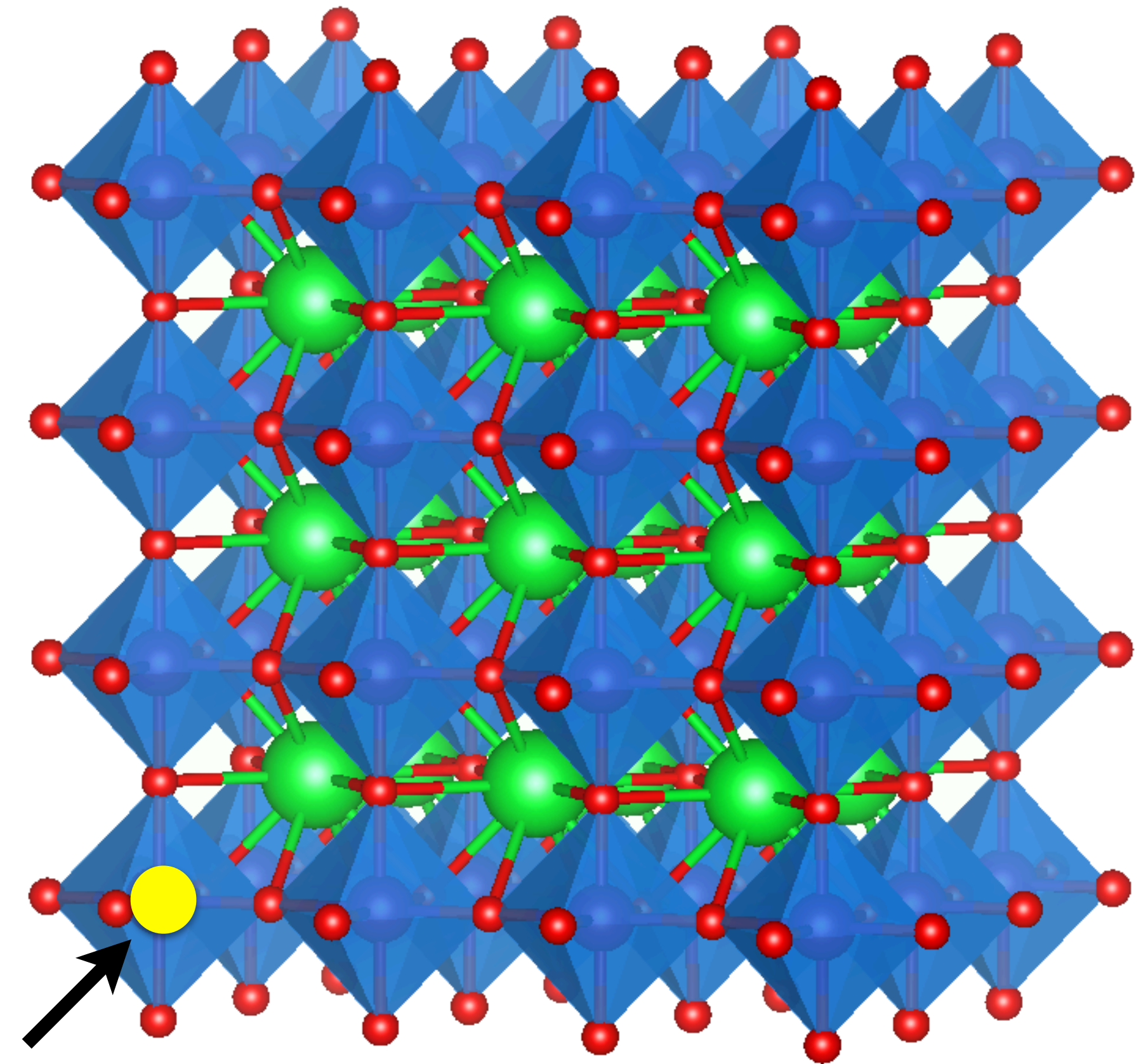
$$\hat{V}_{\text{pert}}^J = \sum_m |\varphi_m^J\rangle \langle \varphi_m^J|$$

Response matrices
(numerical derivative using finite differences)

$$\chi_{IJ} = \frac{\Delta n^I}{\Delta \lambda^J}$$

Hubbard parameters:

$$U^I = (\chi_0^{-1} - \chi^{-1})_{II} \quad V^{IJ} = (\chi_0^{-1} - \chi^{-1})_{IJ}$$

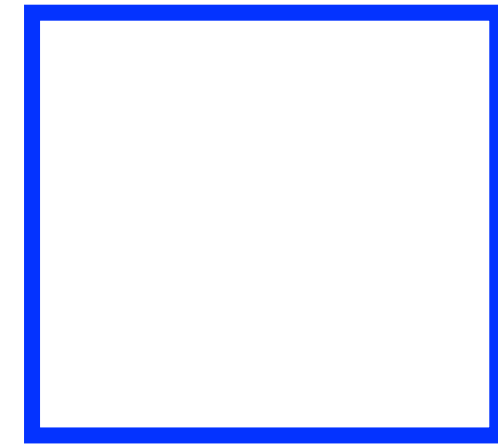


Perturbed
atom

- Computationally expensive
- Possible convergence issues when using large supercells
- Quite cumbersome to use

Link between primitive unit cells and supercells

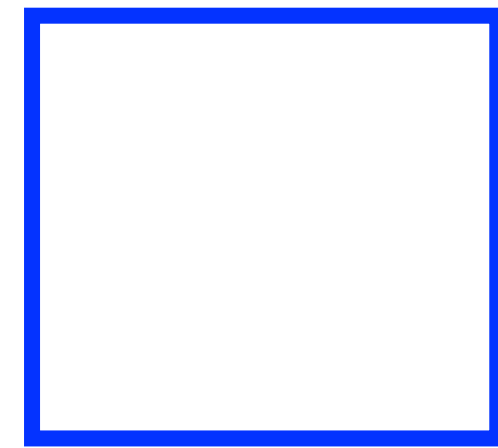
primitive unit cell



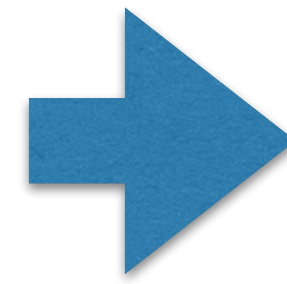
a_i

Link between primitive unit cells and supercells

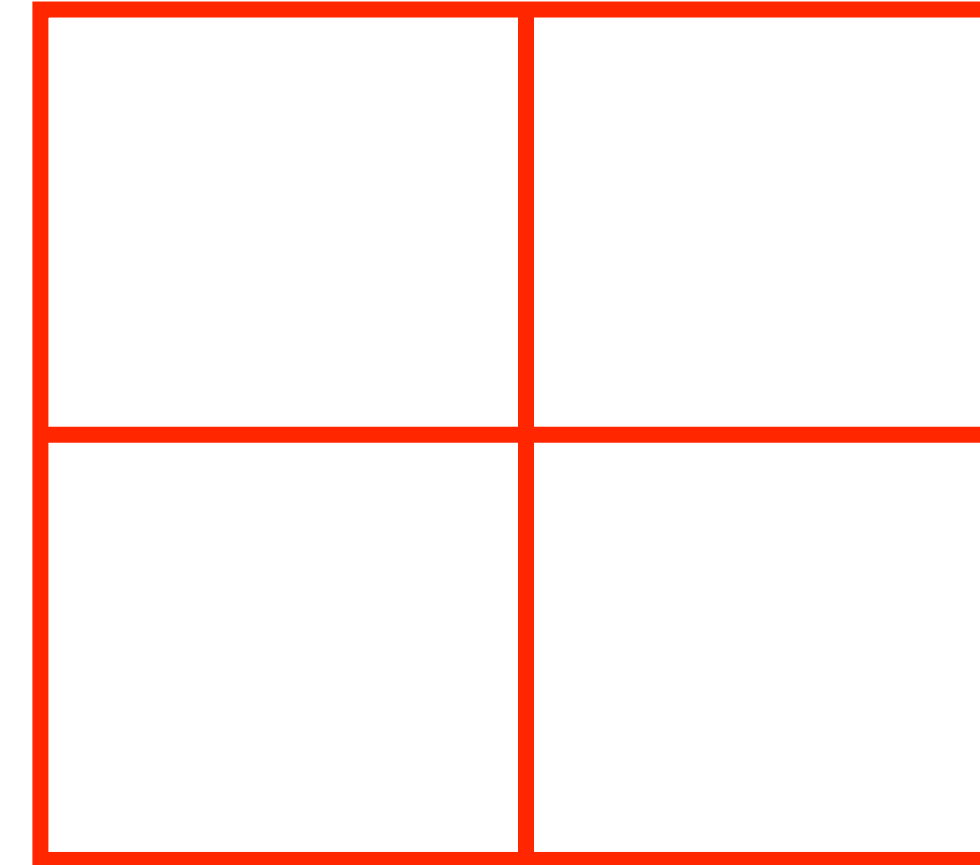
primitive unit cell



\mathbf{a}_i



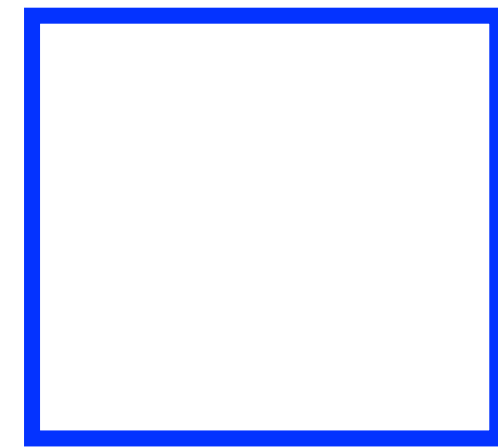
supercell: $L_1 \times L_2 \times L_3$



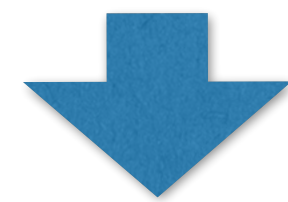
$$\mathbf{A}_i = L_i \mathbf{a}_i$$

Link between primitive unit cells and supercells

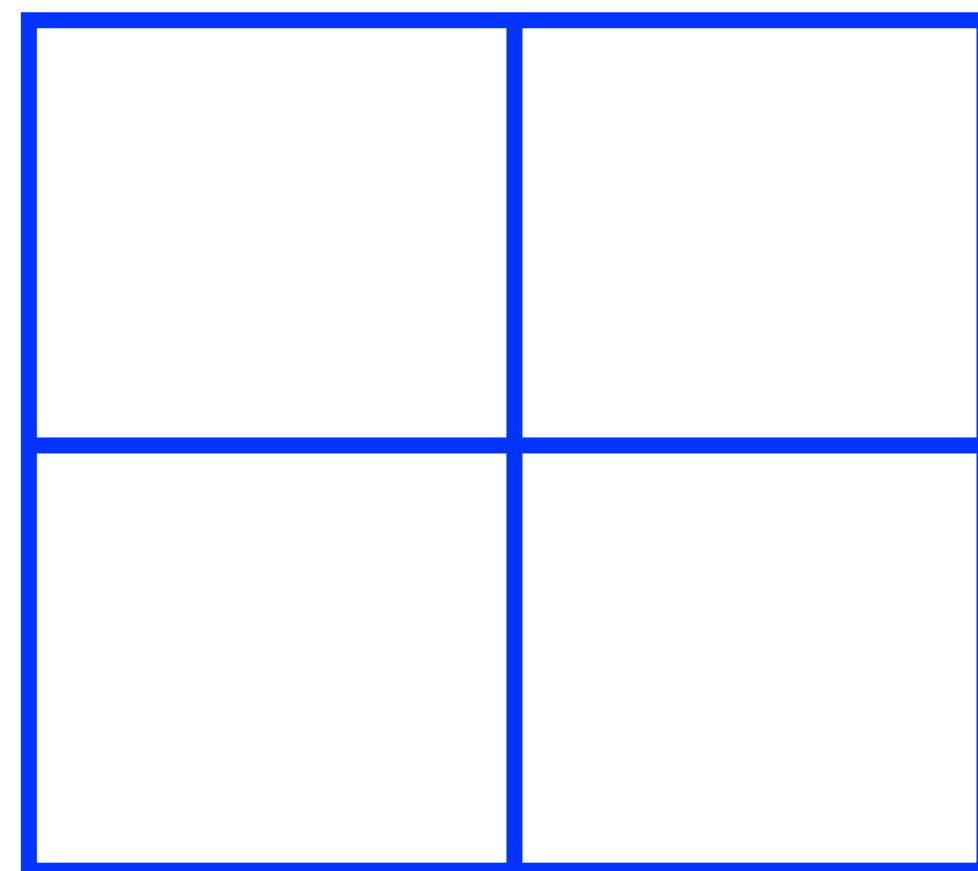
primitive unit cell



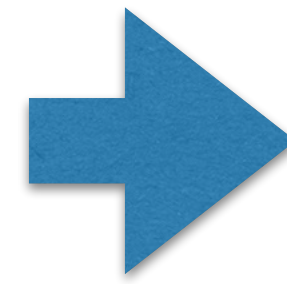
\mathbf{a}_i



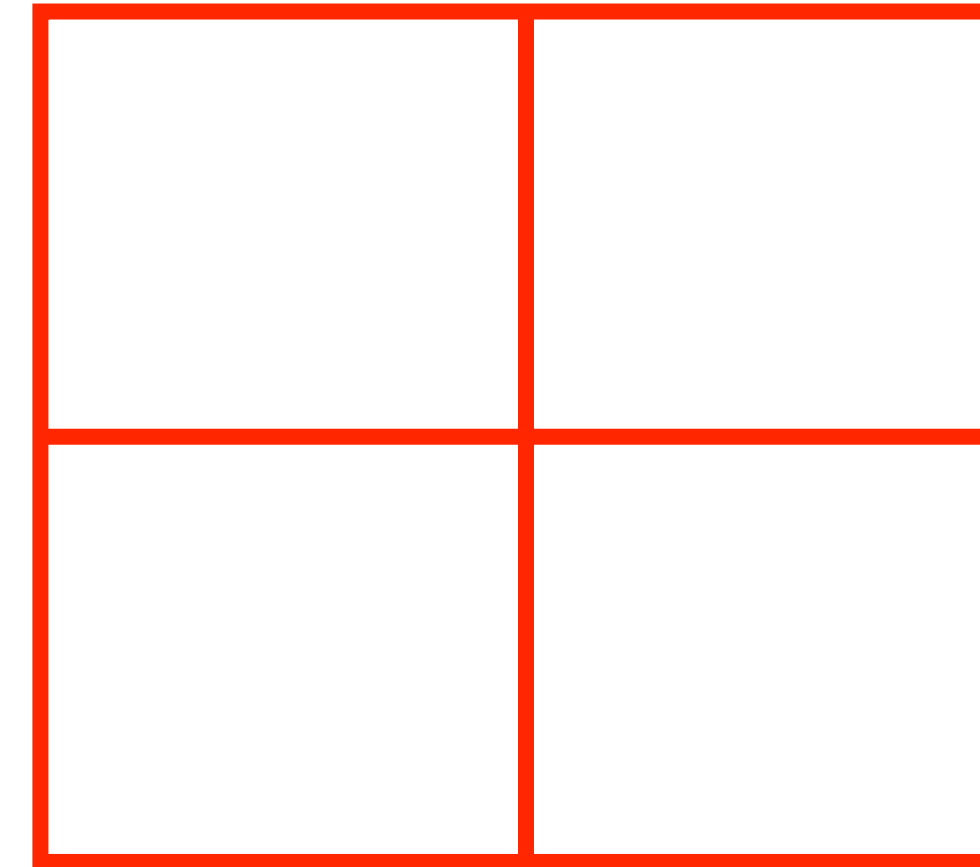
Brillouin zone



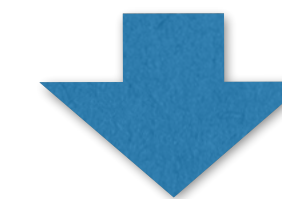
\mathbf{b}_i



supercell: $L_1 \times L_2 \times L_3$



$$\mathbf{A}_i = L_i \mathbf{a}_i$$

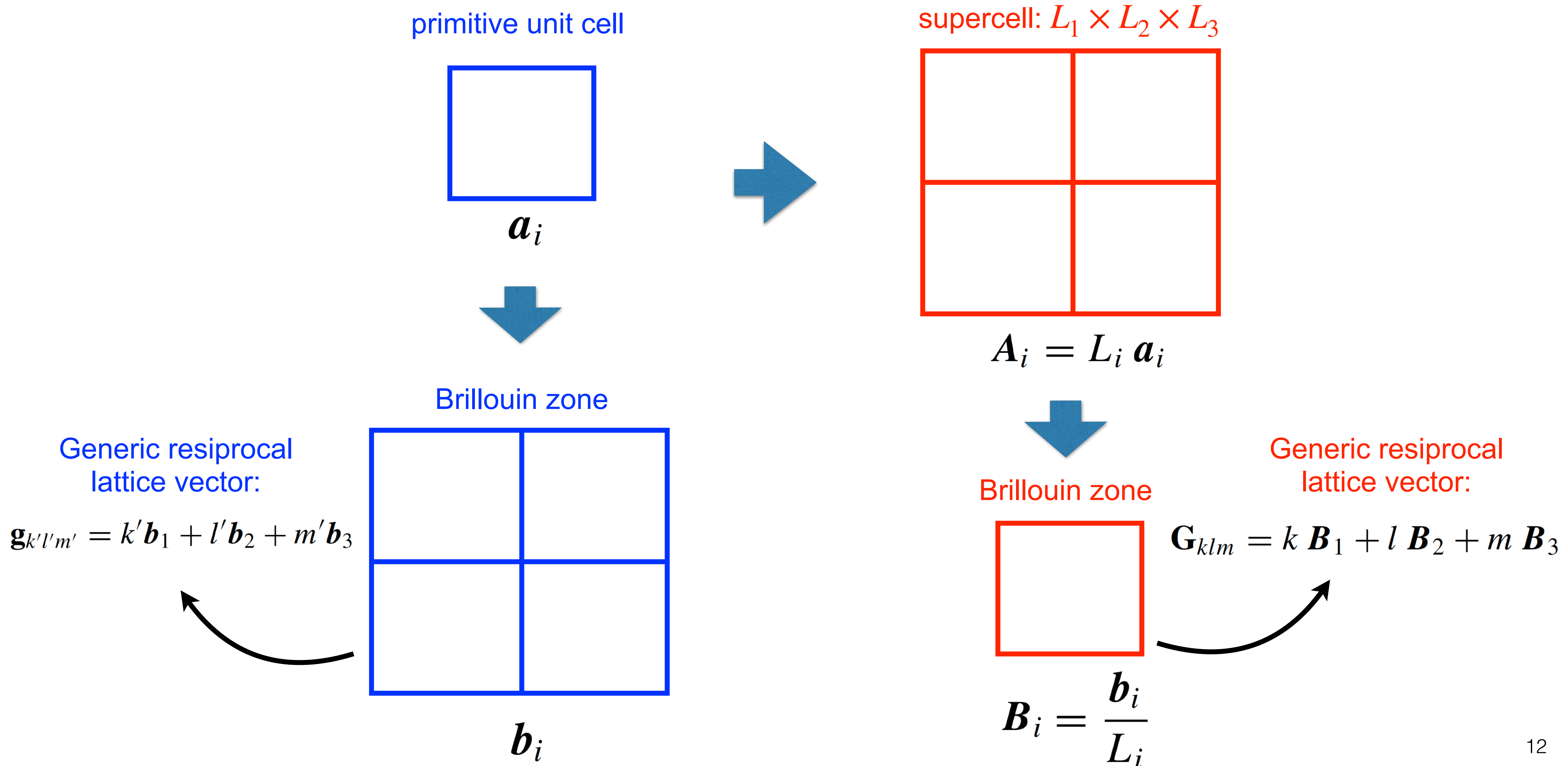


Brillouin zone



$$\mathbf{B}_i = \frac{\mathbf{b}_i}{L_i}$$

Link between primitive unit cells and supercells

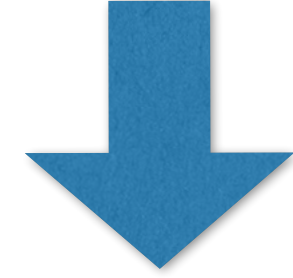


Link between primitive unit cells and supercells

$$\mathbf{G}_{klm} = k \mathbf{B}_1 + l \mathbf{B}_2 + m \mathbf{B}_3$$

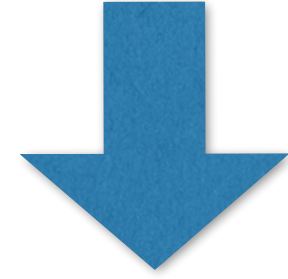
Link between primitive unit cells and supercells

$$\mathbf{G}_{klm} = k \mathbf{B}_1 + l \mathbf{B}_2 + m \mathbf{B}_3$$

 $\mathbf{B}_i = \frac{\mathbf{b}_i}{L_i}$

Link between primitive unit cells and supercells

$$\mathbf{G}_{klm} = k \mathbf{B}_1 + l \mathbf{B}_2 + m \mathbf{B}_3$$

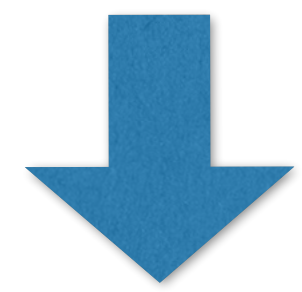


$$\mathbf{B}_i = \frac{\mathbf{b}_i}{L_i}$$

$$\mathbf{G}_{klm} = \frac{k}{L_1} \mathbf{b}_1 + \frac{l}{L_2} \mathbf{b}_2 + \frac{m}{L_3} \mathbf{b}_3$$

Link between primitive unit cells and supercells

$$\mathbf{G}_{klm} = k \mathbf{B}_1 + l \mathbf{B}_2 + m \mathbf{B}_3$$


$$\mathbf{B}_i = \frac{\mathbf{b}_i}{L_i}$$

$$\mathbf{G}_{klm} = \frac{k}{L_1} \mathbf{b}_1 + \frac{l}{L_2} \mathbf{b}_2 + \frac{m}{L_3} \mathbf{b}_3$$

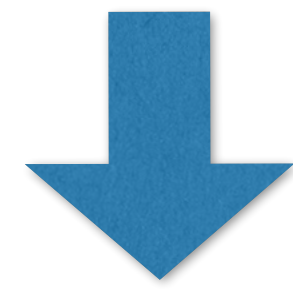
$$k = k' L_1 + \bar{k},$$

$$l = l' L_2 + \bar{l},$$

$$m = m' L_3 + \bar{m}.$$

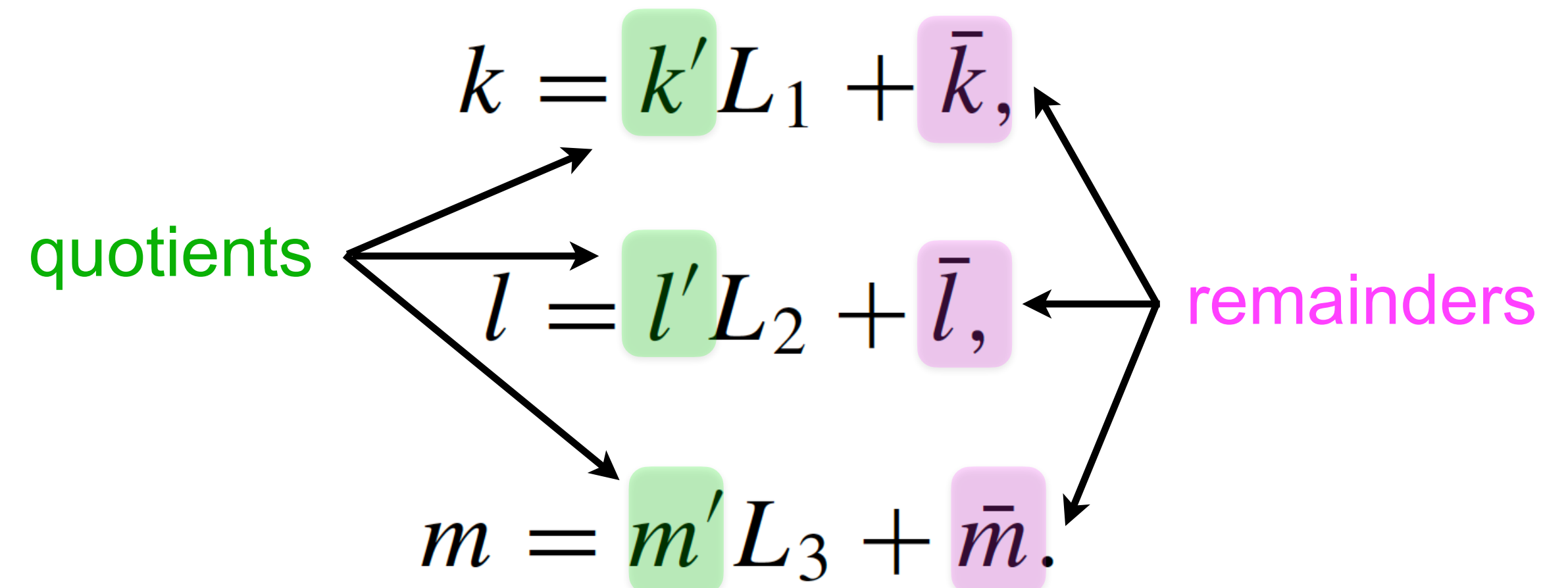
Link between primitive unit cells and supercells

$$\mathbf{G}_{klm} = k \mathbf{B}_1 + l \mathbf{B}_2 + m \mathbf{B}_3$$



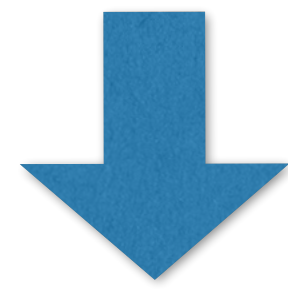
$$\mathbf{B}_i = \frac{\mathbf{b}_i}{L_i}$$

$$\mathbf{G}_{klm} = \frac{k}{L_1} \mathbf{b}_1 + \frac{l}{L_2} \mathbf{b}_2 + \frac{m}{L_3} \mathbf{b}_3$$



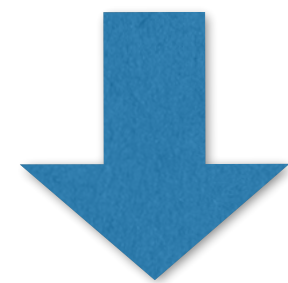
Link between primitive unit cells and supercells

$$\mathbf{G}_{klm} = k \mathbf{B}_1 + l \mathbf{B}_2 + m \mathbf{B}_3$$



$$\mathbf{B}_i = \frac{\mathbf{b}_i}{L_i}$$

$$\mathbf{G}_{klm} = \frac{k}{L_1} \mathbf{b}_1 + \frac{l}{L_2} \mathbf{b}_2 + \frac{m}{L_3} \mathbf{b}_3$$



$$\mathbf{G}_{klm} = \mathbf{g}_{k'l'm'} + \mathbf{q}_{\bar{k}\bar{l}\bar{m}}$$

quotients

$$\begin{aligned} k &= k' L_1 + \bar{k}, \\ l &= l' L_2 + \bar{l}, \\ m &= m' L_3 + \bar{m}. \end{aligned}$$

remainders

$$\mathbf{g}_{k'l'm'} = k' \mathbf{b}_1 + l' \mathbf{b}_2 + m' \mathbf{b}_3$$

$$\mathbf{q}_{\bar{k}\bar{l}\bar{m}} = \frac{\bar{k}}{L_1} \mathbf{b}_1 + \frac{\bar{l}}{L_2} \mathbf{b}_2 + \frac{\bar{m}}{L_3} \mathbf{b}_3$$

Link between primitive unit cells and supercells

Fourier expansion of the perturbing localized potential in a supercell:

$$\begin{aligned} V(\mathbf{r}) &= \sum_{\mathbf{G}} e^{i\mathbf{G}\cdot\mathbf{r}} V(\mathbf{G}) \\ &\equiv \sum_{klm} e^{i\mathbf{G}_{klm}\cdot\mathbf{r}} V(\mathbf{G}_{klm}) \end{aligned}$$

Link between primitive unit cells and supercells

Fourier expansion of the perturbing localized potential in a supercell:

$$\begin{aligned} V(\mathbf{r}) &= \sum_{\mathbf{G}} e^{i\mathbf{G}\cdot\mathbf{r}} V(\mathbf{G}) \\ &\equiv \sum_{klm} e^{i\mathbf{G}_{klm}\cdot\mathbf{r}} V(\mathbf{G}_{klm}) \end{aligned}$$

We can rewrite this potential as a sum of monochromatic perturbations ($\mathbf{G} = \mathbf{g} + \mathbf{q}$):

$$\begin{aligned} V(\mathbf{r}) &= \sum_{\bar{k}\bar{l}\bar{m}} \sum_{k'l'm'} e^{i(\mathbf{g}_{k'l'm'} + \mathbf{q}_{\bar{k}\bar{l}\bar{m}})\cdot\mathbf{r}} V(\mathbf{g}_{k'l'm'} + \mathbf{q}_{\bar{k}\bar{l}\bar{m}}) \\ &\equiv \sum_{\mathbf{q}} \sum_{\mathbf{g}} e^{i(\mathbf{g} + \mathbf{q})\cdot\mathbf{r}} V(\mathbf{g} + \mathbf{q}) \\ &= \sum_{\mathbf{q}} e^{i\mathbf{q}\cdot\mathbf{r}} \bar{V}_{\mathbf{q}}(\mathbf{r}). \end{aligned}$$

$$\bar{V}_{\mathbf{q}}(\mathbf{r}) = \sum_{\mathbf{g}} e^{i\mathbf{g}\cdot\mathbf{r}} V(\mathbf{g} + \mathbf{q})$$

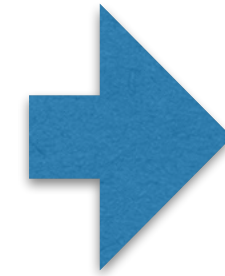
LRT: from supercells to primitive unit cells

Modified Kohn-Sham equations:

$$\left(\hat{H}_\sigma + \lambda^J \hat{V}_{\text{pert}}^J \right) |\psi_{v\mathbf{k}\sigma}\rangle = \varepsilon_{v\mathbf{k}\sigma} |\psi_{v\mathbf{k}\sigma}\rangle$$

Perturbing potential:

$$\hat{V}_{\text{pert}}^J = \sum_m |\varphi_m^J\rangle \langle \varphi_m^J|$$



Perturbation theory to 1st order:

$$\begin{aligned} & \left(\hat{H}_\sigma^\circ - \varepsilon_{v\mathbf{k}\sigma}^\circ \right) \left| \frac{d\psi_{v\mathbf{k}\sigma}}{d\lambda^J} \right\rangle \\ &= - \left(\frac{d\hat{V}_{\text{Hxc},\sigma}}{d\lambda^J} - \frac{d\varepsilon_{v\mathbf{k}\sigma}}{d\lambda^J} + \hat{V}_{\text{pert}}^J \right) |\psi_{v\mathbf{k}\sigma}^\circ\rangle \end{aligned}$$

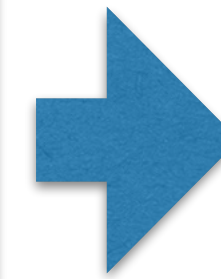
LRT: from supercells to primitive unit cells

Modified Kohn-Sham equations:

$$\left(\hat{H}_\sigma + \lambda^J \hat{V}_{\text{pert}}^J \right) |\psi_{v\mathbf{k}\sigma}\rangle = \varepsilon_{v\mathbf{k}\sigma} |\psi_{v\mathbf{k}\sigma}\rangle$$

Perturbing potential:

$$\hat{V}_{\text{pert}}^J = \sum_m |\varphi_m^J\rangle \langle \varphi_m^J|$$



Perturbation theory to 1st order:

$$\begin{aligned} & \left(\hat{H}_\sigma^\circ - \varepsilon_{v\mathbf{k}\sigma}^\circ \right) \left| \frac{d\psi_{v\mathbf{k}\sigma}}{d\lambda^J} \right\rangle \\ &= - \left(\frac{d\hat{V}_{\text{Hxc},\sigma}}{d\lambda^J} - \frac{d\varepsilon_{v\mathbf{k}\sigma}}{d\lambda^J} + \hat{V}_{\text{pert}}^J \right) |\psi_{v\mathbf{k}\sigma}^\circ\rangle \end{aligned}$$

Potential in a supercell can be decomposed into a sum over \mathbf{q} points for a primitive cell:

$$V(\mathbf{r}) = \sum_{\mathbf{q}} e^{i\mathbf{q}\cdot\mathbf{r}} \bar{V}_{\mathbf{q}}(\mathbf{r})$$

LRT: from supercells to primitive unit cells

Modified Kohn-Sham equations:

$$\left(\hat{H}_\sigma + \lambda^J \hat{V}_{\text{pert}}^J \right) |\psi_{v\mathbf{k}\sigma}\rangle = \varepsilon_{v\mathbf{k}\sigma} |\psi_{v\mathbf{k}\sigma}\rangle$$

Perturbing potential:

$$\hat{V}_{\text{pert}}^J = \sum_m |\varphi_m^J\rangle \langle \varphi_m^J|$$

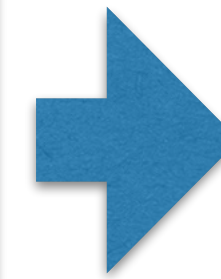
Response matrices

(numerical derivative using finite differences)

$$\chi_{IJ} = \frac{\Delta n^I}{\Delta \lambda^J}$$

Hubbard parameters:

$$U^I = (\chi_0^{-1} - \chi^{-1})_{II} \quad V^{IJ} = (\chi_0^{-1} - \chi^{-1})_{IJ}$$



Perturbation theory to 1st order:

$$\begin{aligned} & (\hat{H}_\sigma^\circ - \varepsilon_{v\mathbf{k}\sigma}^\circ) \left| \frac{d\psi_{v\mathbf{k}\sigma}}{d\lambda^J} \right\rangle \\ &= - \left(\frac{d\hat{V}_{\text{Hxc},\sigma}}{d\lambda^J} - \frac{d\varepsilon_{v\mathbf{k}\sigma}}{d\lambda^J} + \hat{V}_{\text{pert}}^J \right) |\psi_{v\mathbf{k}\sigma}^\circ\rangle \end{aligned}$$

Potential in a supercell can be decomposed into a sum over \mathbf{q} points for a primitive cell:

$$V(\mathbf{r}) = \sum_{\mathbf{q}} e^{i\mathbf{q}\cdot\mathbf{r}} \bar{V}_{\mathbf{q}}(\mathbf{r})$$

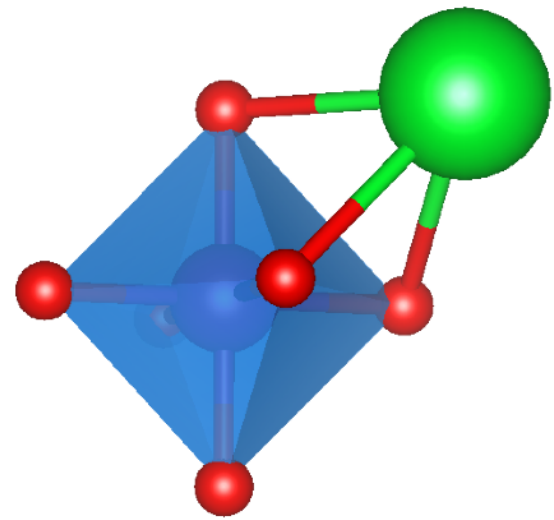
Response occupation matrices (from the iterative solution of the eq. above)

$$\frac{dn_{m_1 m_2}^{s\sigma}}{d\lambda^{s'l'}} = \frac{1}{N_{\mathbf{q}}} \sum_{\mathbf{q}} e^{i\mathbf{q}\cdot(\mathbf{R}_l - \mathbf{R}_{l'})} \Delta_{\mathbf{q}}^{s'} \bar{n}_{m_1 m_2}^{s\sigma}$$

LRT: from supercells to primitive unit cells

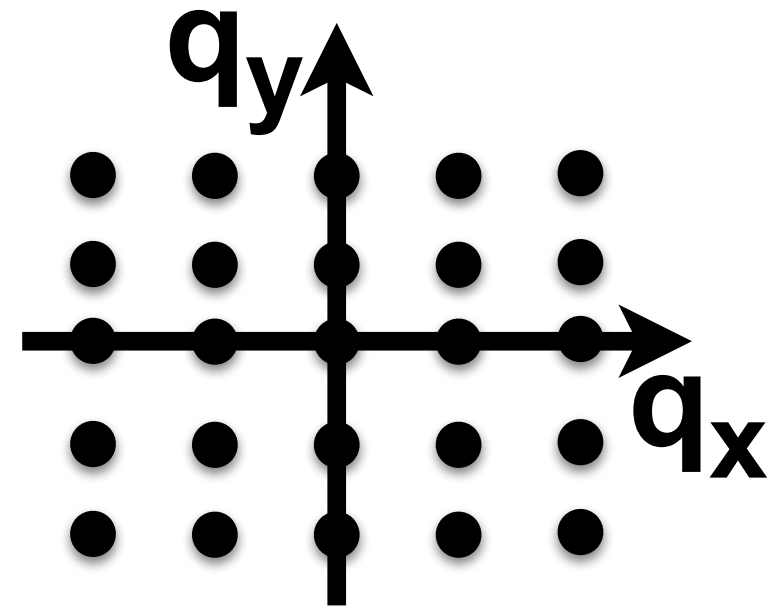
Density-functional perturbation theory (DFPT)

primitive cell



+

monochromatic perturbations



- Computationally much less expensive
- Easier convergence
- User-friendly and autonomous

Inspired by DFPT for phonons:

Baroni, de Gironcoli, Dal Corso, Giannozzi, RMP (2001).

Timrov, Marzari, and Cococcioni, Phys. Rev. B (2018) & (2021).

Perturbation theory to 1st order:

$$\begin{aligned} & (\hat{H}_\sigma^\circ - \varepsilon_{v\mathbf{k}\sigma}^\circ) \left| \frac{d\psi_{v\mathbf{k}\sigma}}{d\lambda^J} \right\rangle \\ &= - \left(\frac{d\hat{V}_{\text{Hxc},\sigma}}{d\lambda^J} - \frac{d\varepsilon_{v\mathbf{k}\sigma}}{d\lambda^J} + \hat{V}_{\text{pert}}^J \right) |\psi_{v\mathbf{k}\sigma}^\circ\rangle \end{aligned}$$

Potential in a supercell can be decomposed into a sum over \mathbf{q} points for a primitive cell:

$$V(\mathbf{r}) = \sum_{\mathbf{q}} e^{i\mathbf{q}\cdot\mathbf{r}} \bar{V}_{\mathbf{q}}(\mathbf{r})$$

Response occupation matrices
(from the iterative solution of the eq. above)

$$\frac{dn_{m_1 m_2}^{s\sigma}}{d\lambda^{s'l'}} = \frac{1}{N_{\mathbf{q}}} \sum_{\mathbf{q}} e^{i\mathbf{q}\cdot(\mathbf{R}_l - \mathbf{R}_{l'})} \Delta_{\mathbf{q}}^{s'} \bar{n}_{m_1 m_2}^{s\sigma}$$


Hubbard parameters from DFPT

PHYSICAL REVIEW B **98**, 085127 (2018)

Hubbard parameters from density-functional perturbation theory

Iurii Timrov, Nicola Marzari, and Matteo Cococcioni

*Theory and Simulation of Materials (THEOS) and National Centre for Computational Design and Discovery of Novel Materials (MARVEL),
École Polytechnique Fédérale de Lausanne (EPFL), CH-1015 Lausanne, Switzerland*

 (Received 4 May 2018; revised manuscript received 27 July 2018; published 16 August 2018)

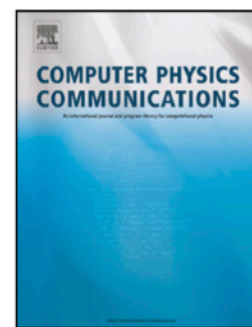
Computer Physics Communications 279 (2022) 108455






Contents lists available at [ScienceDirect](https://www.sciencedirect.com)

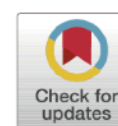
Computer Physics Communications

www.elsevier.com/locate/cpc





HP – A code for the calculation of Hubbard parameters using density-functional perturbation theory   

Iurii Timrov ^{a,*}, Nicola Marzari ^{a,b}, Matteo Cococcioni ^c




PHYSICAL REVIEW B **103**, 045141 (2021)

Self-consistent Hubbard parameters from density-functional perturbation theory in the ultrasoft and projector-augmented wave formulations

Iurii Timrov ^{1,*}, Nicola Marzari ¹ and Matteo Cococcioni²

¹*Theory and Simulation of Materials (THEOS), and National Centre for Computational Design and Discovery of Novel Materials (MARVEL),
École Polytechnique Fédérale de Lausanne (EPFL), CH-1015 Lausanne, Switzerland*

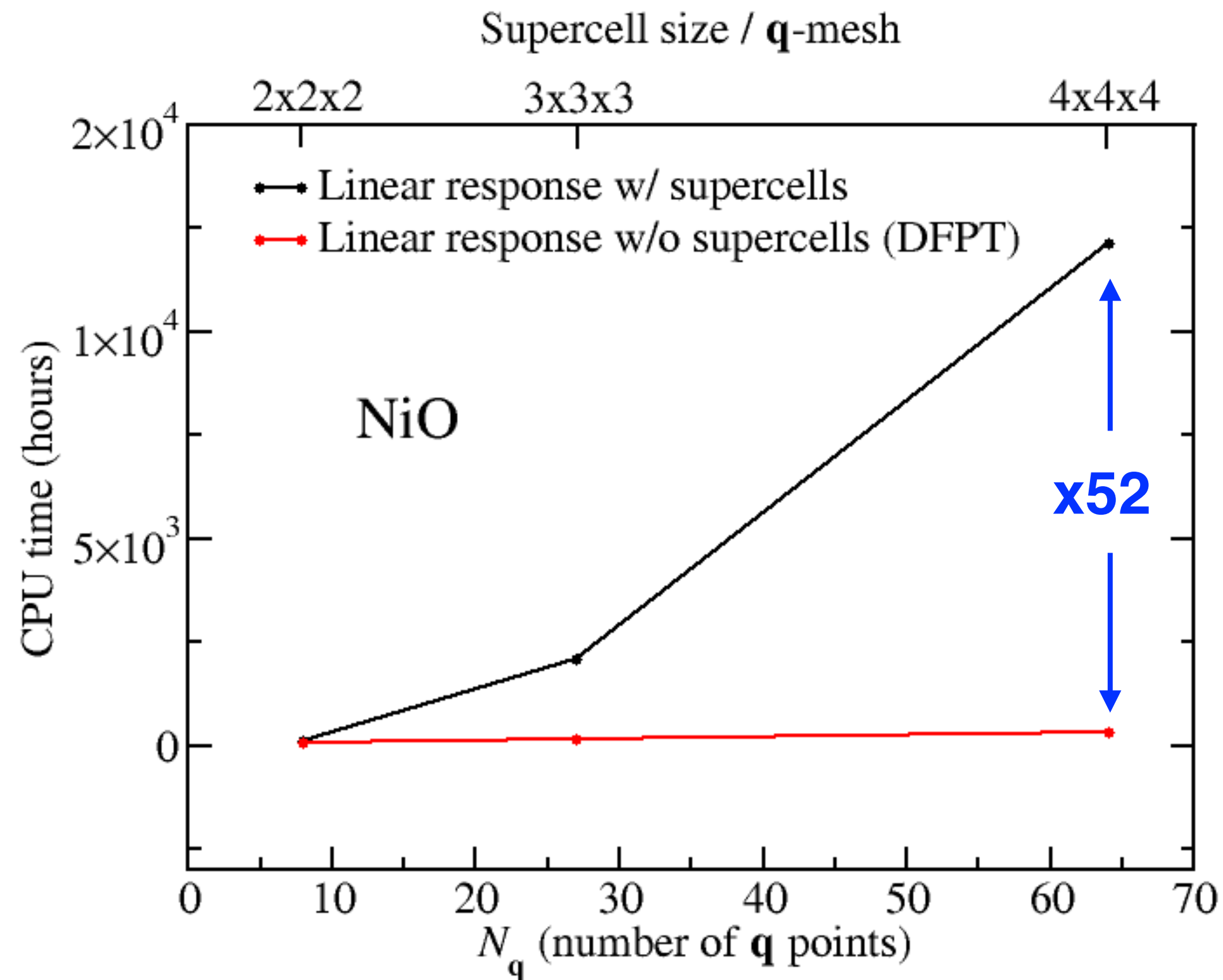
²*Department of Physics, University of Pavia, via Bassi 6, I-27100 Pavia, Italy*

 (Received 6 November 2020; accepted 14 January 2021; published 29 January 2021)



Numerical comparison of U from LRT and DFPT

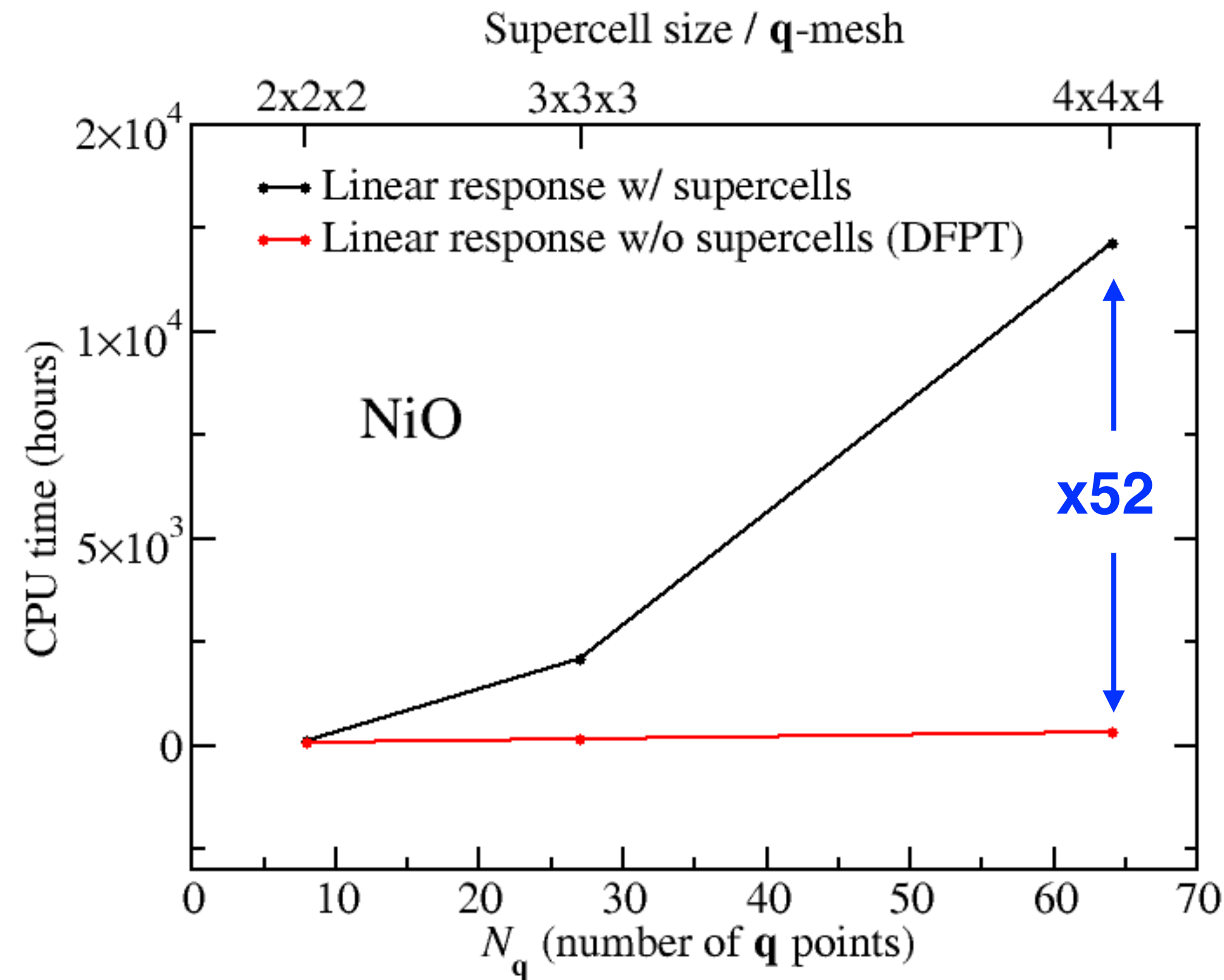
Scaling



Symmetry → Reduction of $N_{\mathbf{q}}$ in DFPT
(no equivalence in the SC approach)

Numerical comparison of U from LRT and DFPT

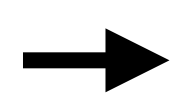
Scaling



Benchmark of the equivalence between the two approaches

Method	\mathbf{k} -mesh	SC-size/ \mathbf{q} -mesh	$U(\text{Ni-}d)$
LR-SC	$6 \times 6 \times 6$	$2 \times 2 \times 2$	7.895
DFPT	$12 \times 12 \times 12$		7.900
LR-SC	$4 \times 4 \times 4$	$3 \times 3 \times 3$	8.146
DFPT	$12 \times 12 \times 12$		8.149
LR-SC	$3 \times 3 \times 3$	$4 \times 4 \times 4$	8.168
DFPT	$12 \times 12 \times 12$		8.172

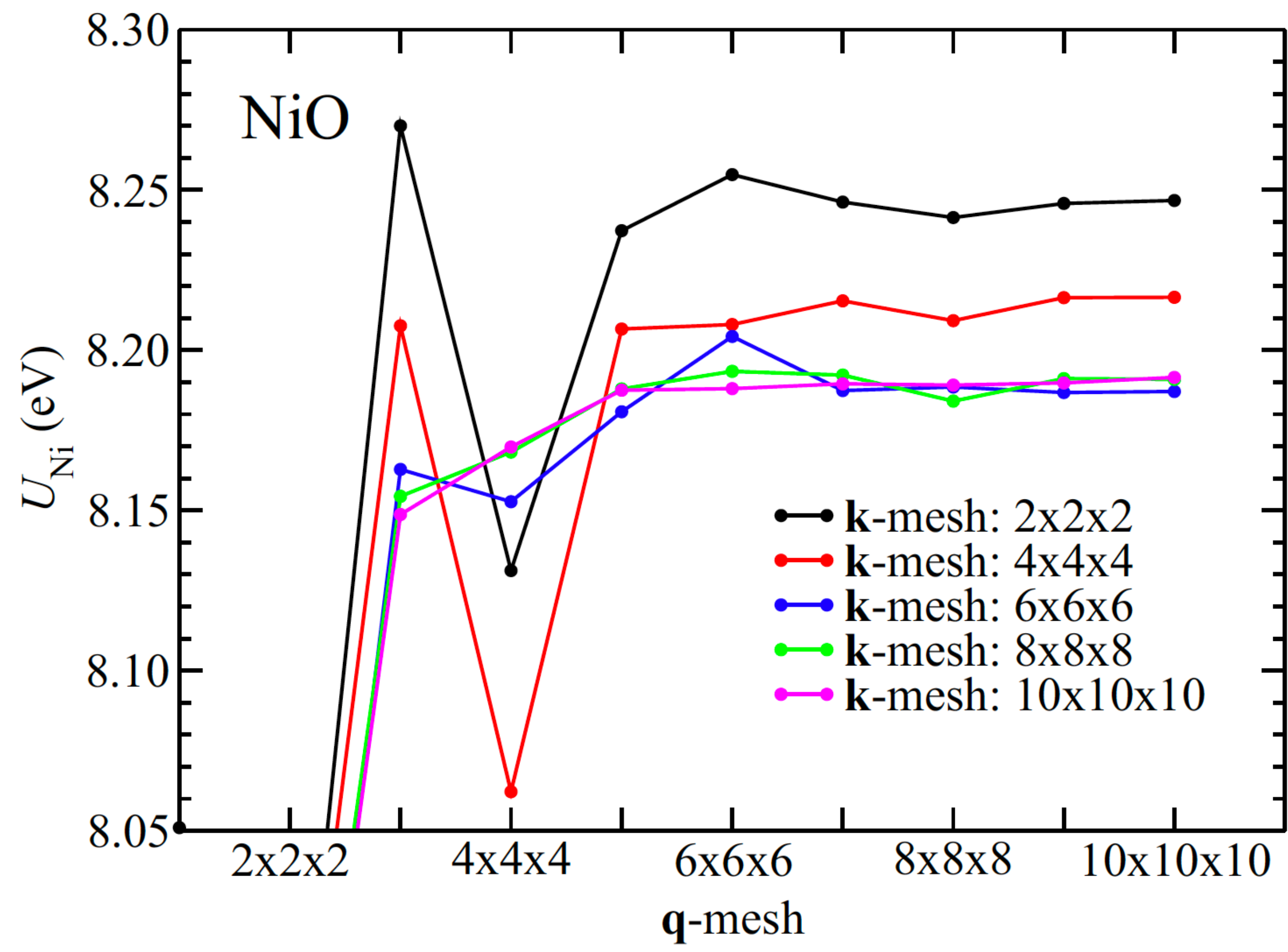
Symmetry



Reduction of $N_{\mathbf{q}}$ in DFPT
(no equivalence in the SC approach)

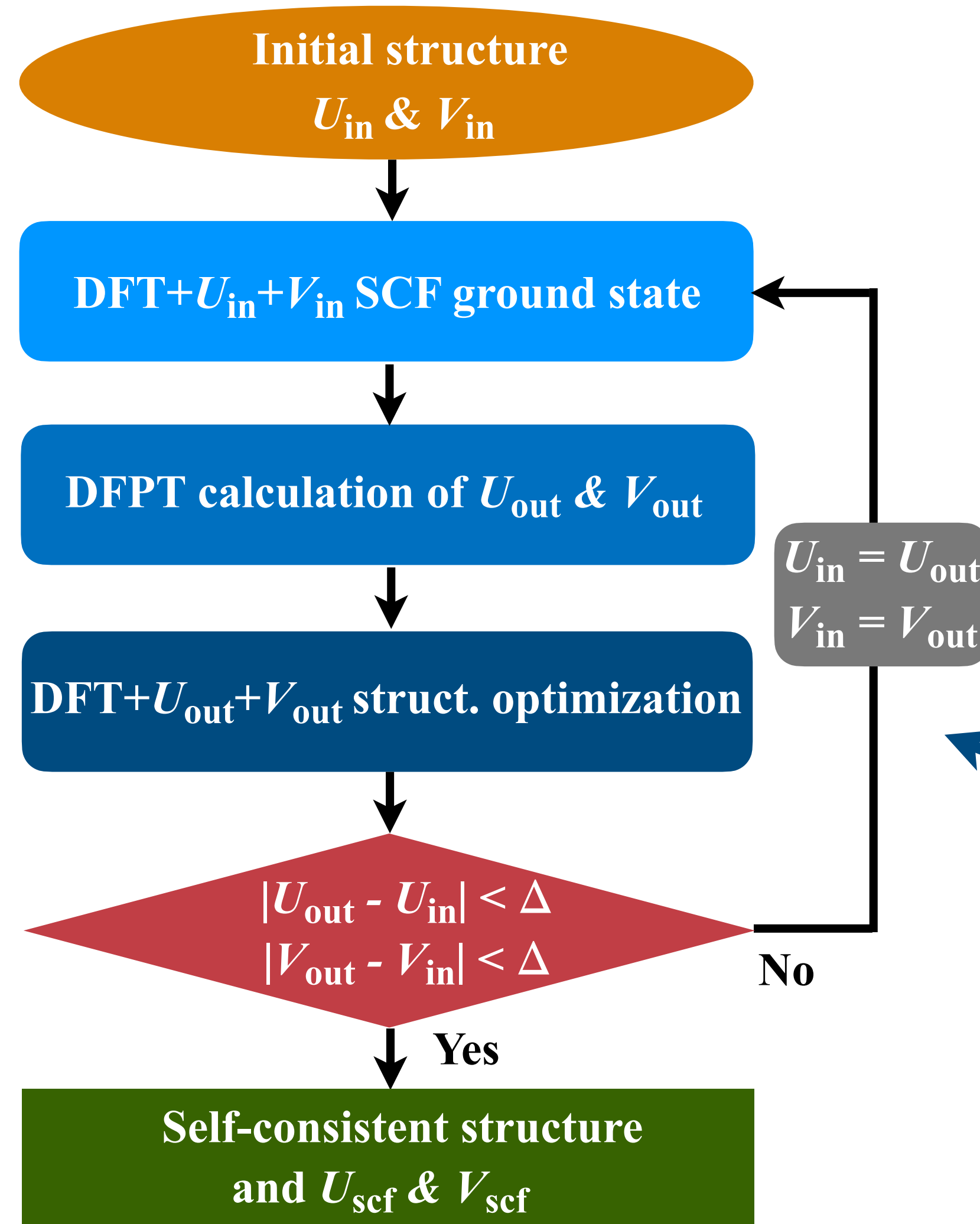
Exact matching
(modulo the numerical noise)

Convergence of U with respect to k and q points meshes within DFPT



The converged U value is ~ 8.18 eV.

Self-consistent workflow for computing U and V

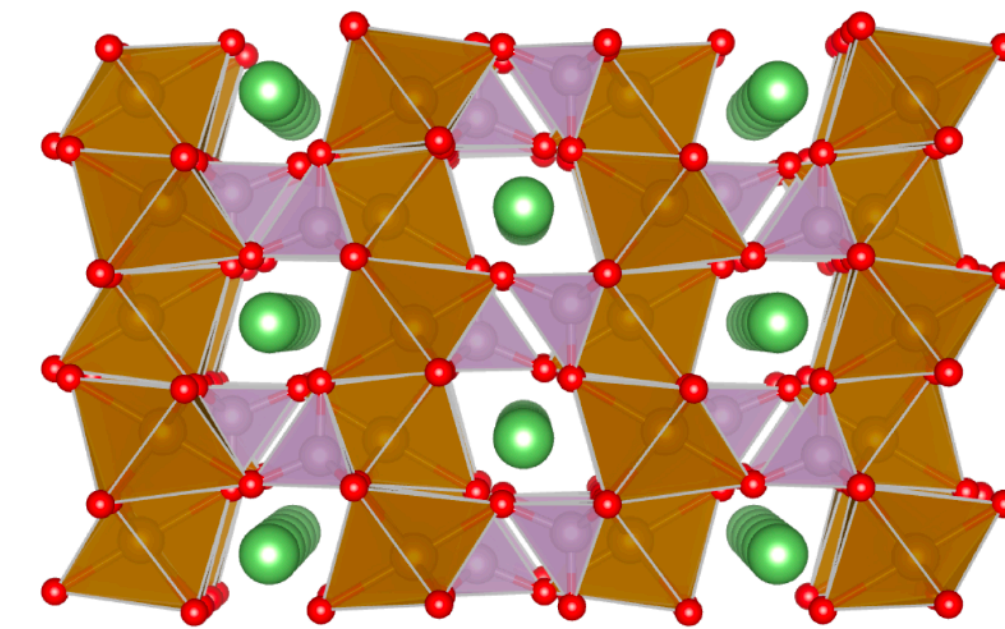


Calculation of Hubbard parameters

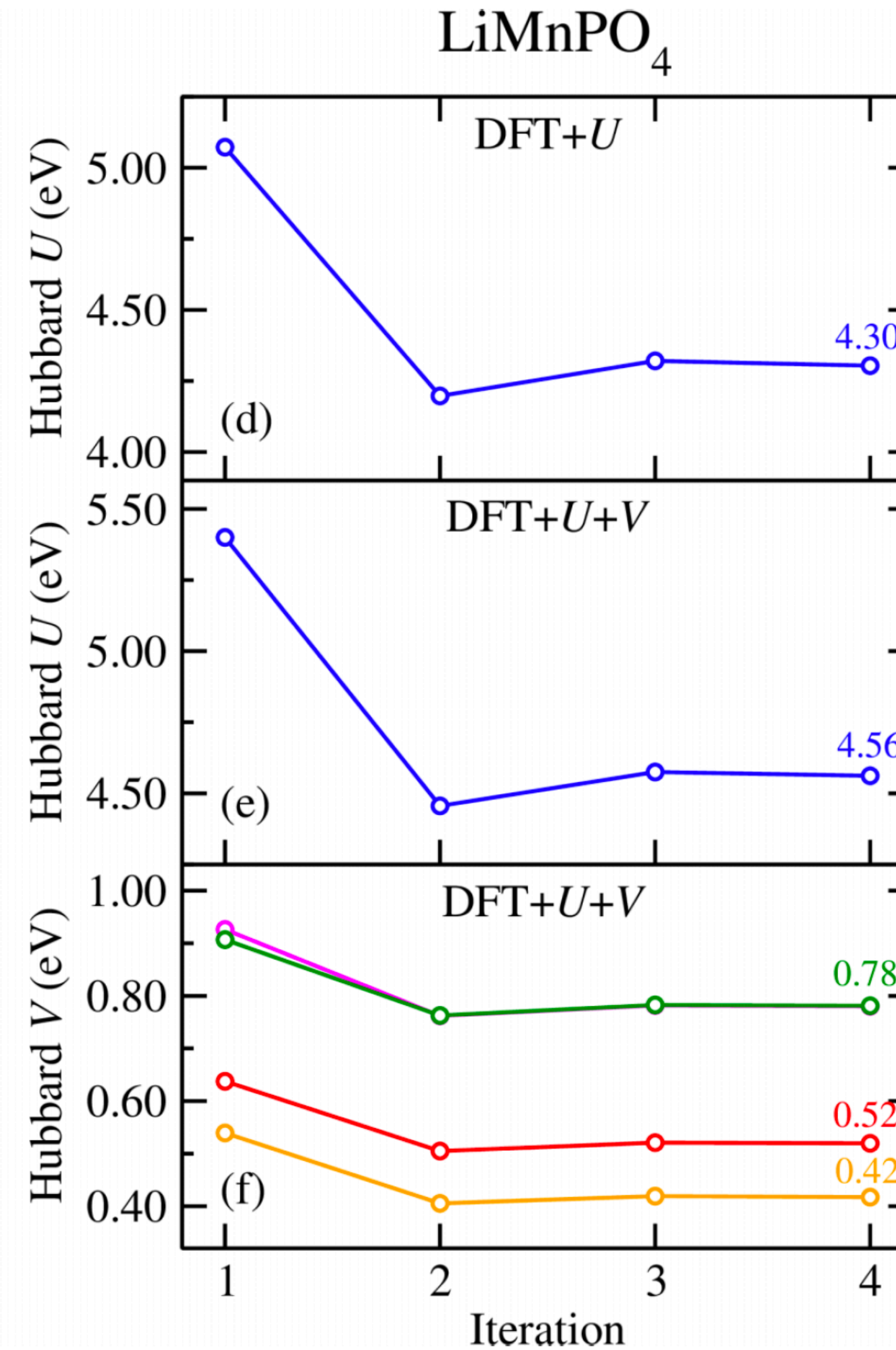
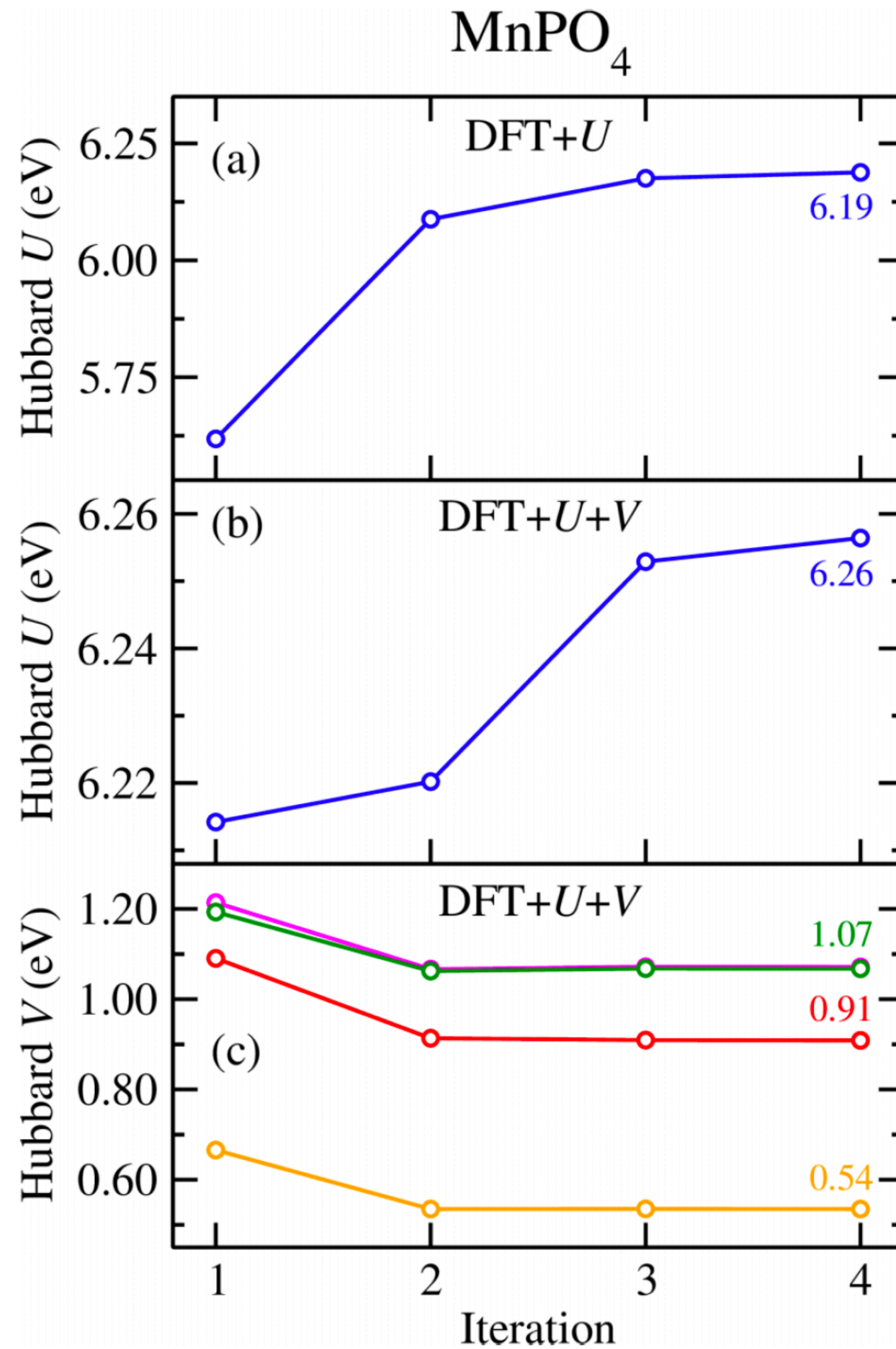
$$U^I = \left(\frac{d^2 E_{\text{DFT}}}{dn^2} - \frac{d^2 E_{\text{DFT}}^\circ}{dn^2} \right)_{II}$$

$$V^{IJ} = \left(\frac{d^2 E_{\text{DFT}}}{dn^2} - \frac{d^2 E_{\text{DFT}}^\circ}{dn^2} \right)_{IJ}$$

Structural optimisation



Self-consistent Hubbard parameters



Types of Hubbard projector functions

1. Nonorthogonalized atomic orbitals (NAO)

$$\phi_{m_1}^I(\mathbf{r} - \mathbf{R}_I) \quad (\text{contained in pseudopotentials})$$

2. Orthogonalized atomic orbitals (OAO)

$$\tilde{\phi}_{m_1}^I(\mathbf{r} - \mathbf{R}_I) = \sum_{Jm_2} \left(\hat{O}^{-\frac{1}{2}} \right)_{m_2m_1}^{JI} \phi_{m_2}^J(\mathbf{r} - \mathbf{R}_J)$$

$$\left(\hat{O} \right)_{m_1m_2}^{IJ} = \langle \phi_{m_1}^I | \phi_{m_2}^J \rangle$$

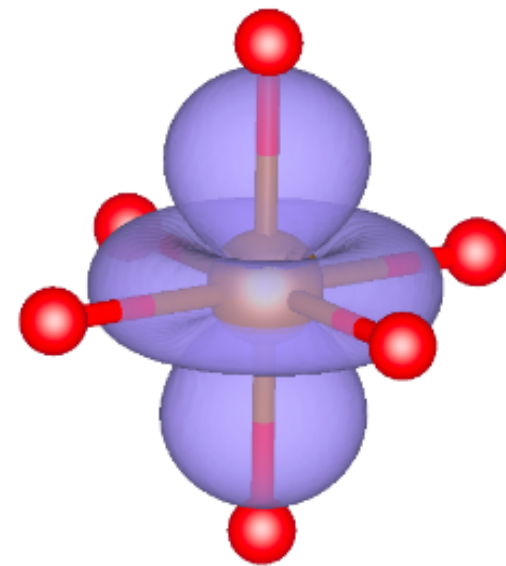
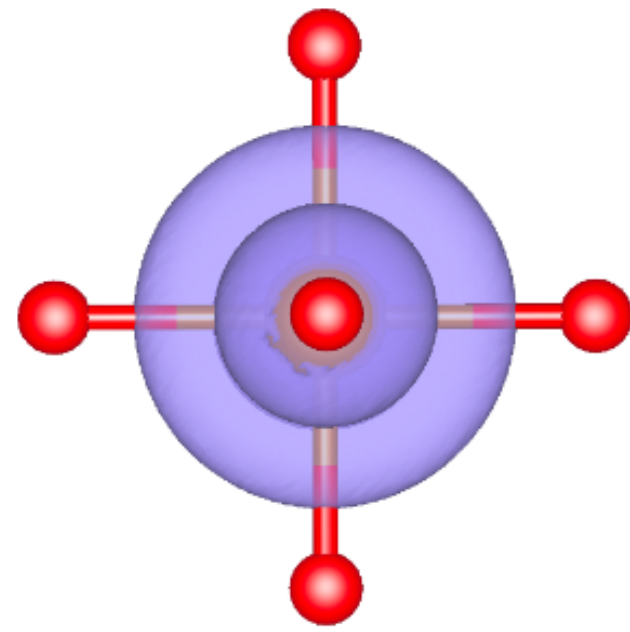
3. Maximally localized Wannier functions (MLWF)

$$w_{m_1}^I(\mathbf{r} - \mathbf{R}_I) = \frac{1}{\sqrt{N_{\mathbf{k}}}} \sum_{\mathbf{k}} e^{-i\mathbf{k} \cdot \mathbf{R}_I} \sum_n^{N_{\text{KSbands}}} U_{nm_1}^{(\mathbf{k})} \psi_{n\mathbf{k}}(\mathbf{r})$$

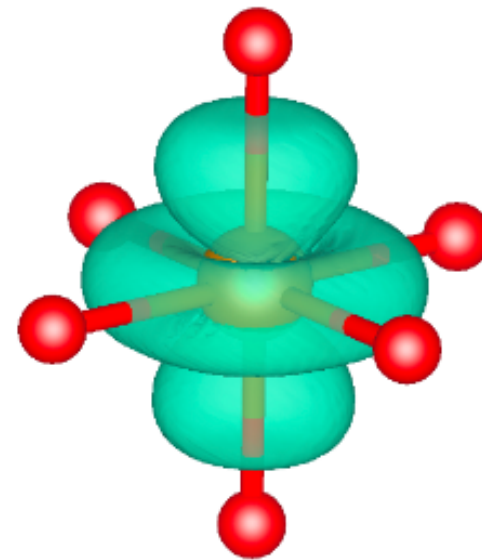
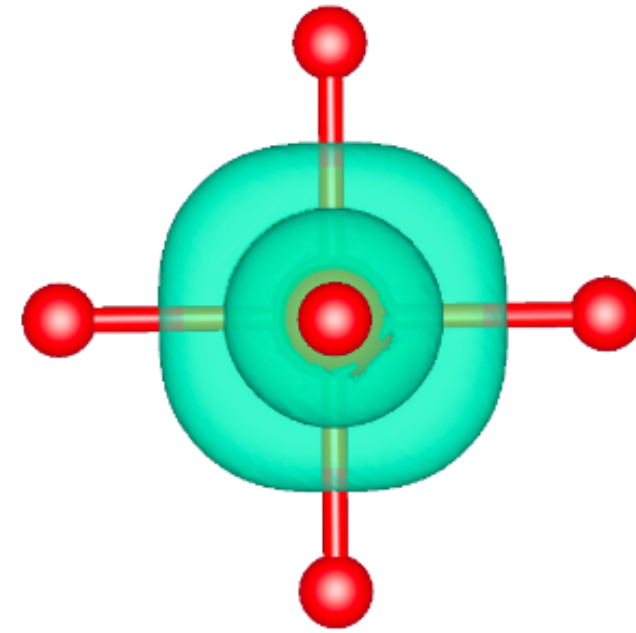
Orthogonalized
Projector
Wannier
wave
functions
plane
augmented
projectors
Linearized
Nonorthogonalized
orbitals

Types of Hubbard projector functions (for FeO)

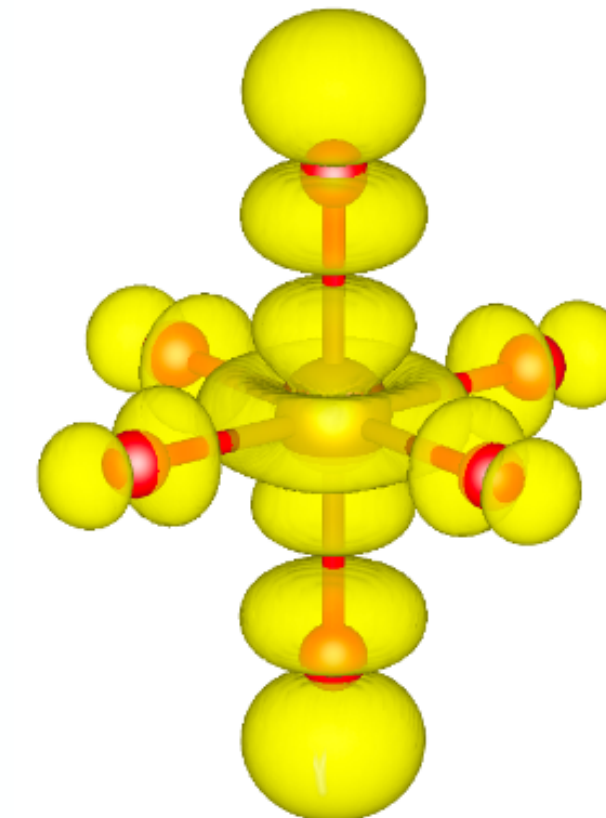
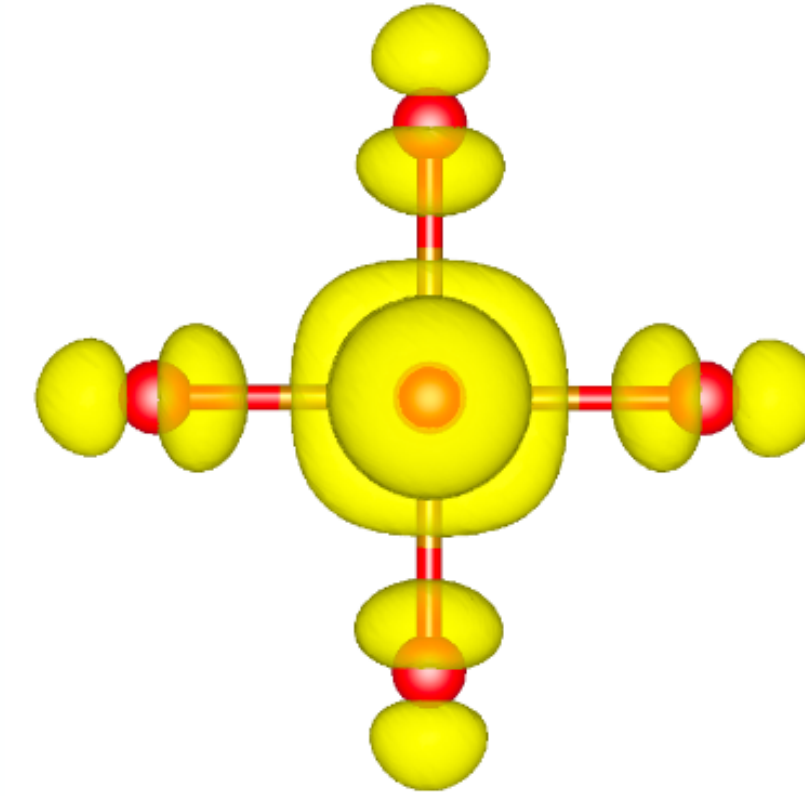
NAO



OAO



MLWFs (frontier)



Types of Hubbard projector functions

1. Nonorthogonalized atomic orbitals (NAO)

$$\phi_{m_1}^I(\mathbf{r} - \mathbf{R}_I) \quad (\text{contained in pseudopotentials})$$

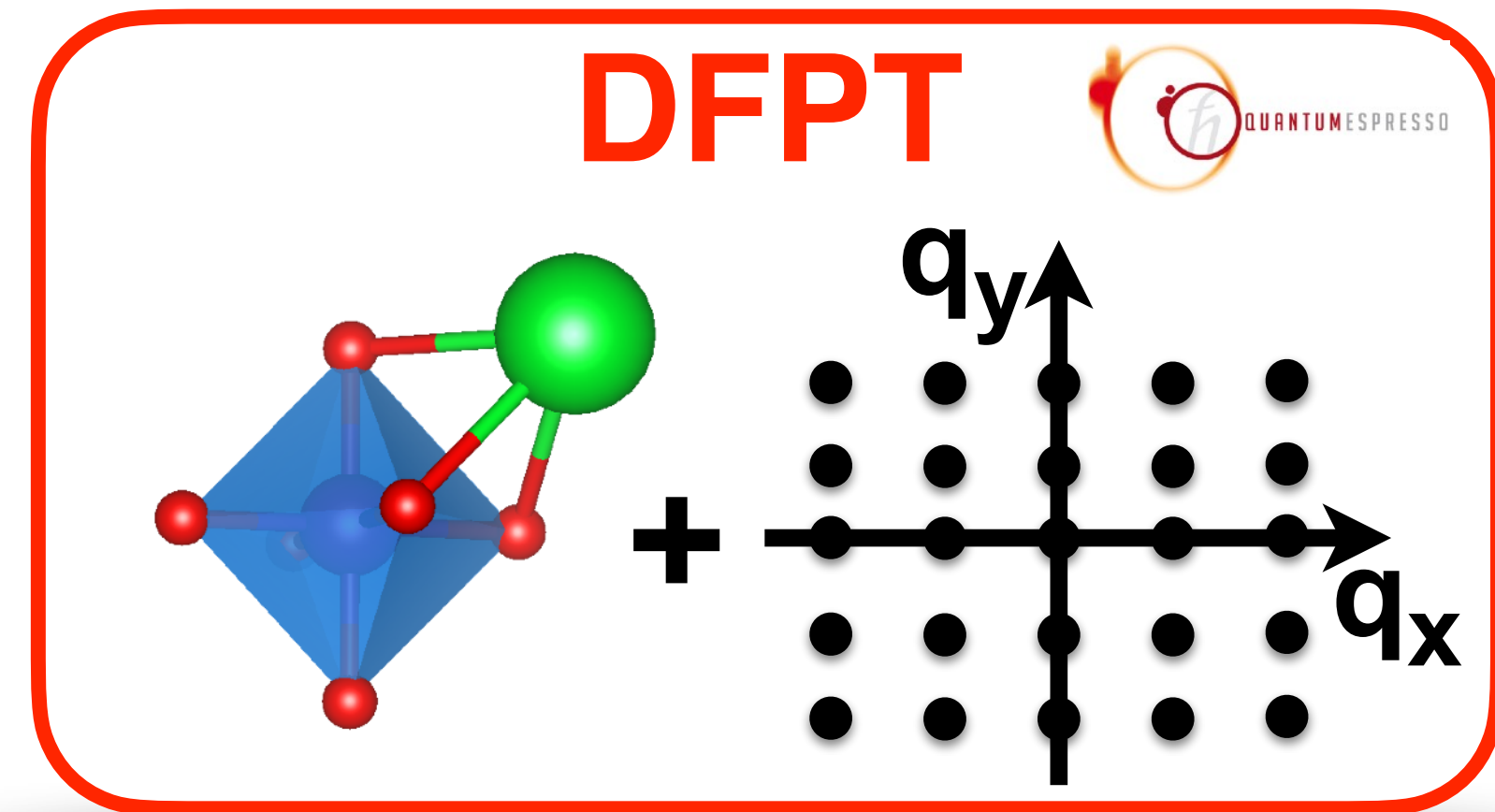
2. Orthogonalized atomic orbitals (OAO)

$$\tilde{\phi}_{m_1}^I(\mathbf{r} - \mathbf{R}_I) = \sum_{Jm_2} \left(\hat{O}^{-\frac{1}{2}} \right)_{m_2m_1}^{JI} \phi_{m_2}^J(\mathbf{r} - \mathbf{R}_J)$$

$$\left(\hat{O} \right)_{m_1m_2}^{IJ} = \langle \phi_{m_1}^I | \phi_{m_2}^J \rangle$$

3. Maximally localized Wannier functions (MLWF)

$$w_{m_1}^I(\mathbf{r} - \mathbf{R}_I) = \frac{1}{\sqrt{N_{\mathbf{k}}}} \sum_{\mathbf{k}} e^{-i\mathbf{k} \cdot \mathbf{R}_I} \sum_n^{N_{\text{KSbands}}} U_{nm_1}^{(\mathbf{k})} \psi_{n\mathbf{k}}(\mathbf{r})$$



U_{atomic}
 V_{atomic}

\neq

U_{ortho}
 V_{ortho}



Types of Hubbard projector functions

1. Nonorthogonalized atomic orbitals (NAO)

$$\phi_{m_1}^I(\mathbf{r} - \mathbf{R}_I) \quad (\text{contained in pseudopotentials})$$

2. Orthogonalized atomic orbitals (OAO)

$$\tilde{\phi}_{m_1}^I(\mathbf{r} - \mathbf{R}_I) = \sum_{Jm_2} \left(\hat{O}^{-\frac{1}{2}} \right)_{m_2m_1}^{JI} \phi_{m_2}^J(\mathbf{r} - \mathbf{R}_J)$$

$$\left(\hat{O} \right)_{m_1m_2}^{IJ} = \langle \phi_{m_1}^I | \phi_{m_2}^J \rangle$$

3. Maximally localized Wannier functions (MLWF)

$$w_{m_1}^I(\mathbf{r} - \mathbf{R}_I) = \frac{1}{\sqrt{N_{\mathbf{k}}}} \sum_{\mathbf{k}} e^{-i\mathbf{k} \cdot \mathbf{R}_I} \sum_n^{N_{\text{KSbands}}} U_{nm_1}^{(\mathbf{k})} \psi_{n\mathbf{k}}(\mathbf{r})$$

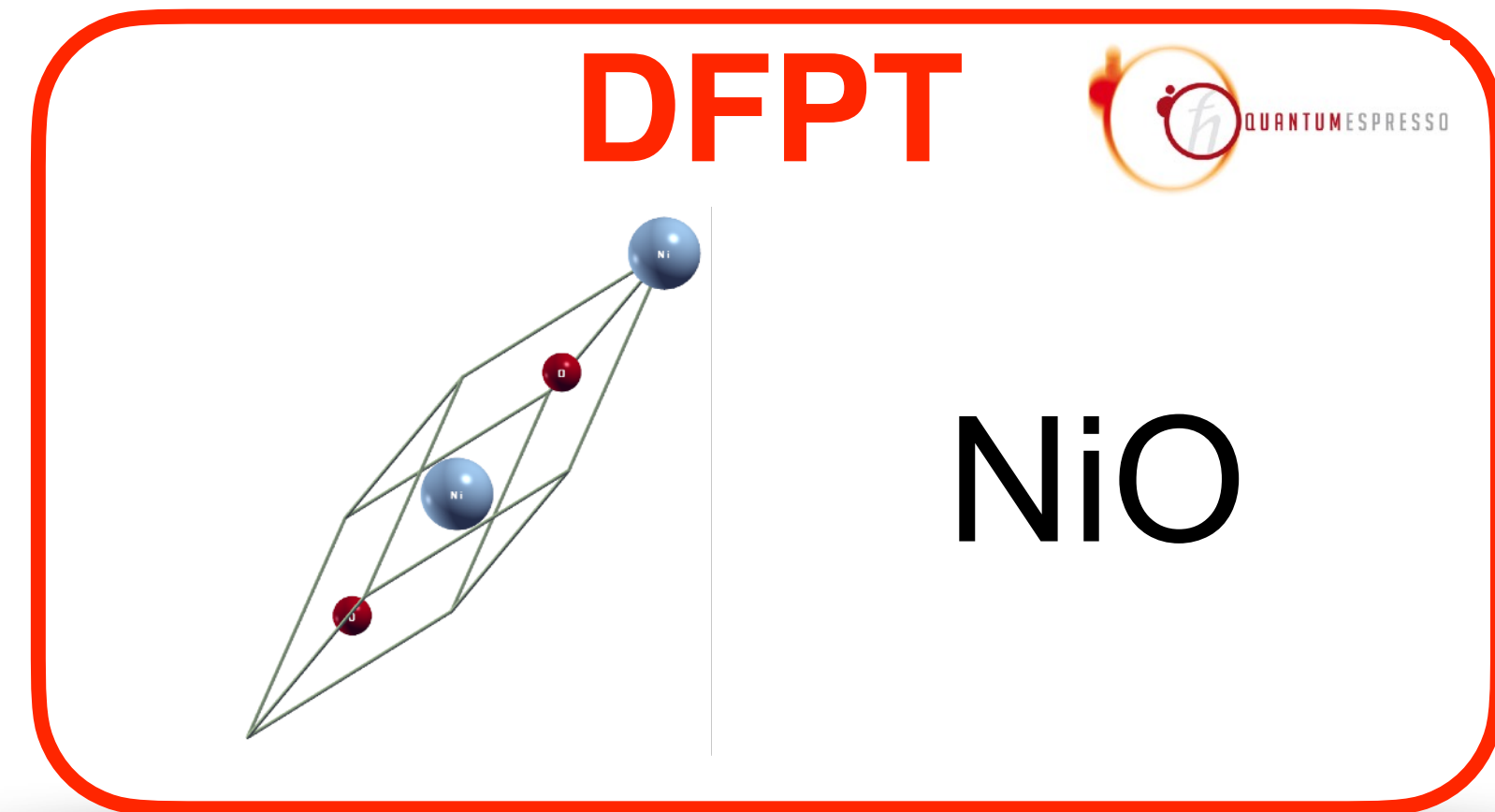
$$U=6.76$$

$$V=1.25$$

≠

$$U=7.43$$

$$V=0.37$$



Types of Hubbard projector functions

1. Nonorthogonalized atomic orbitals

$$\phi_{m_1}^I(\mathbf{r} - \mathbf{R}_I)$$

2. Orthogonalized atomic orbitals

$$\tilde{\phi}_{m_1}^I(\mathbf{r} - \mathbf{R}_I)$$

3. Maximally localized Wannier functions

$$w_{m_1}^I(\mathbf{r} - \mathbf{R}_I) = \frac{1}{\sqrt{N_{\mathbf{k}}}} \sum_{\mathbf{k}} e^{-i\mathbf{k} \cdot \mathbf{R}_I} \sum_n U_{nm_1}^{(\mathbf{k})} \psi_{n\mathbf{k}}(\mathbf{r})$$

It is crucial to keep consistency between Hubbard parameters and Hubbard projectors!

$$U=6.76$$

$$V=1.25$$

\neq

$$U=7.43$$

$$V=0.37$$

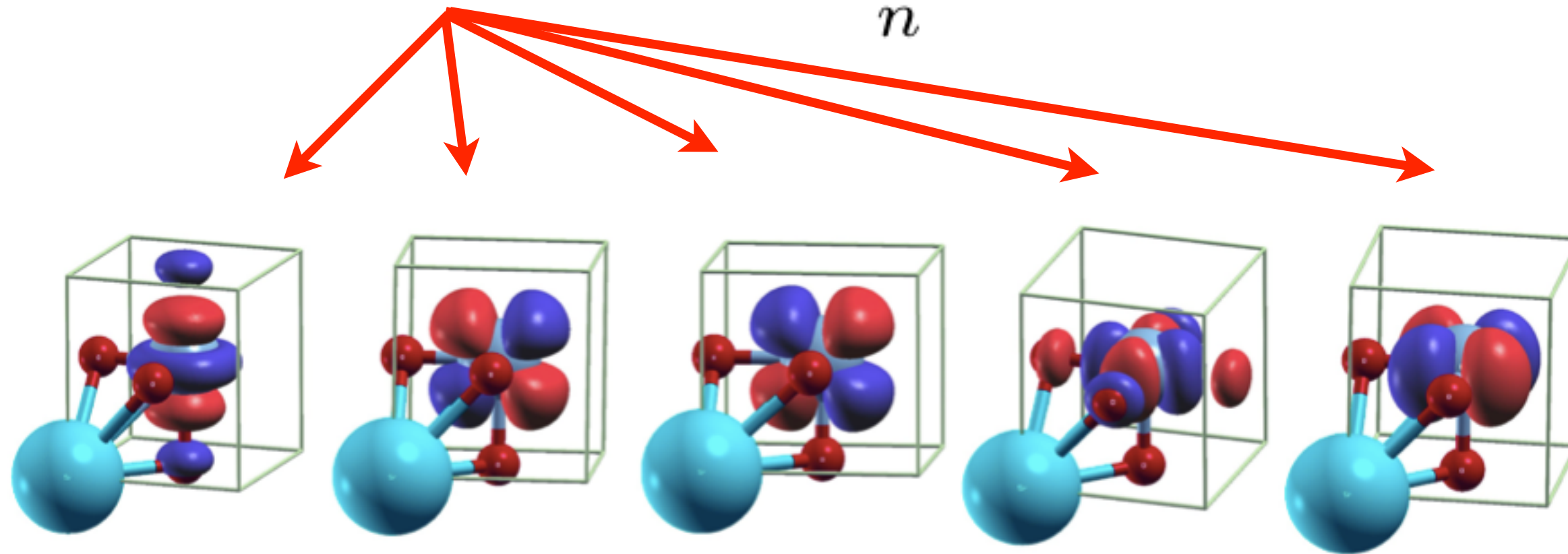


DFT+U with Wannier functions as projectors

WANNIER90



$$\bar{w}_{m,\mathbf{k}}^I(\mathbf{r}) = \sum_n^{N_{\text{KSbands}}} U_{nm}^{(\mathbf{k})} u_{n\mathbf{k}}(\mathbf{r})$$

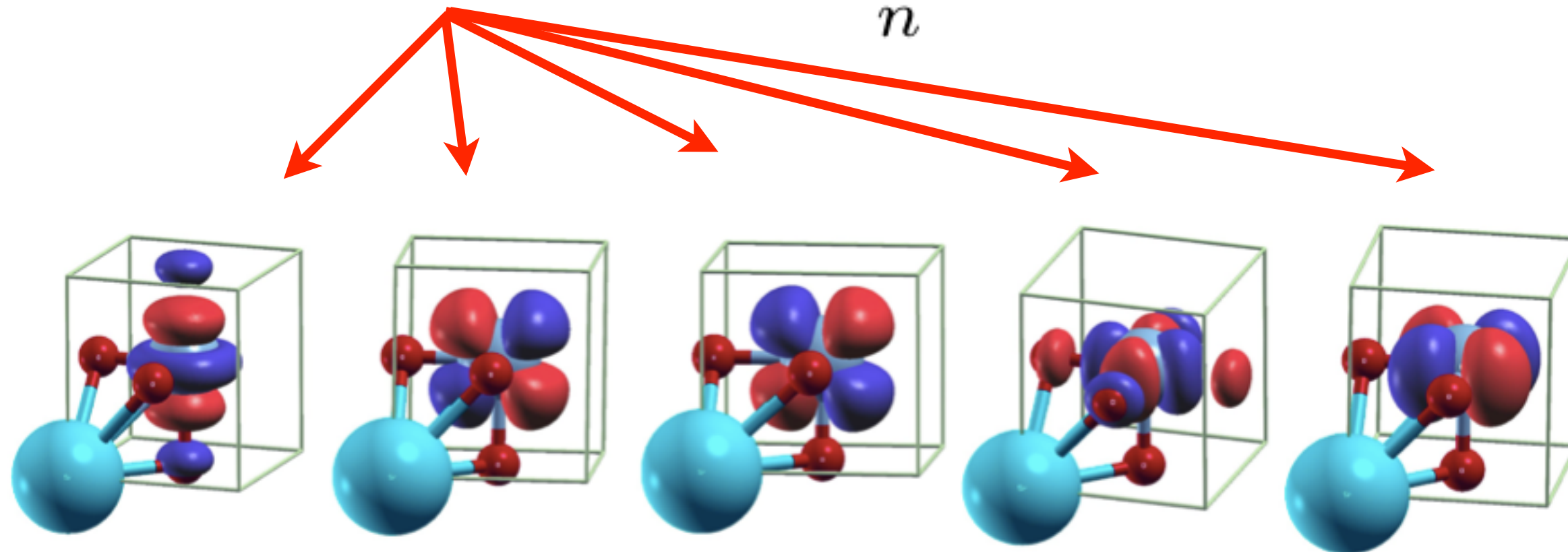


DFT+U with Wannier functions as projectors

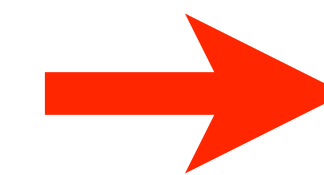
WANNIER90



$$\bar{w}_{m,\mathbf{k}}^I(\mathbf{r}) = \sum_n^{N_{\text{KSbands}}} U_{nm}^{(\mathbf{k})} u_{n\mathbf{k}}(\mathbf{r})$$



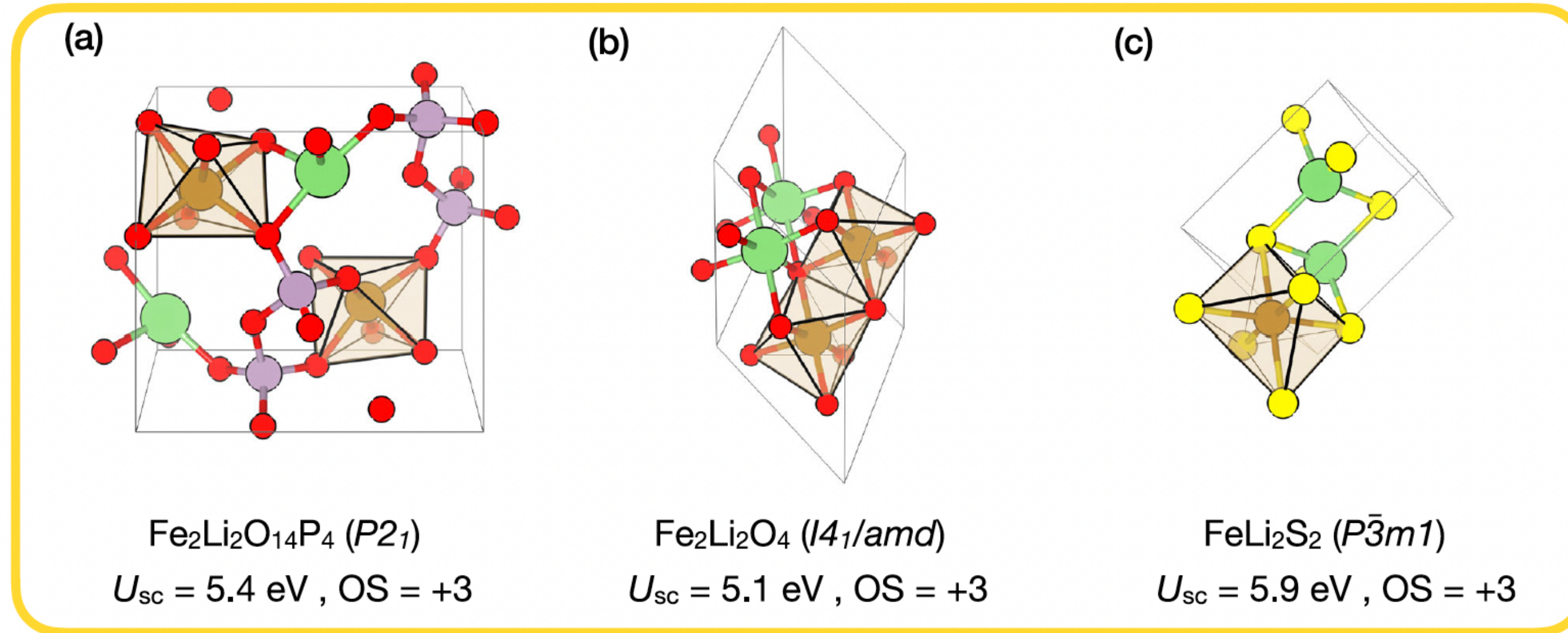
$$n_{m_1 m_2}^I = \frac{1}{N_{\mathbf{k}}} \sum_{v\mathbf{k}} \langle u_{v\mathbf{k}} | \bar{w}_{m_2, \mathbf{k}}^I \rangle \langle \bar{w}_{m_1, \mathbf{k}}^I | u_{v\mathbf{k}} \rangle$$



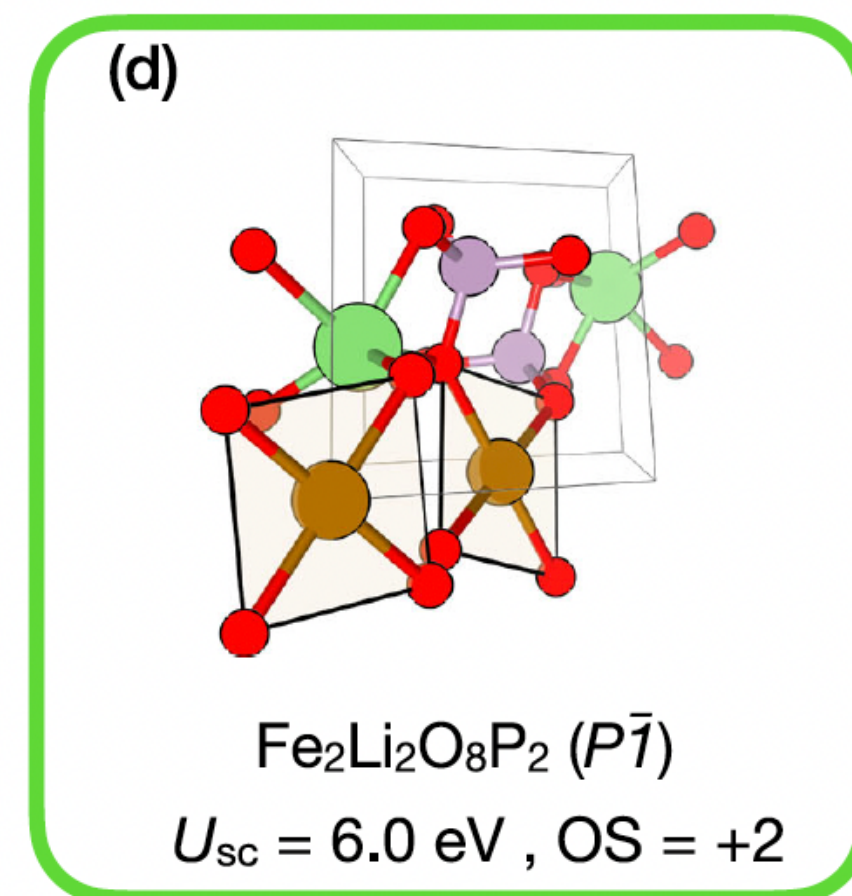
DFT+U

Hubbard parameters depend on many factors

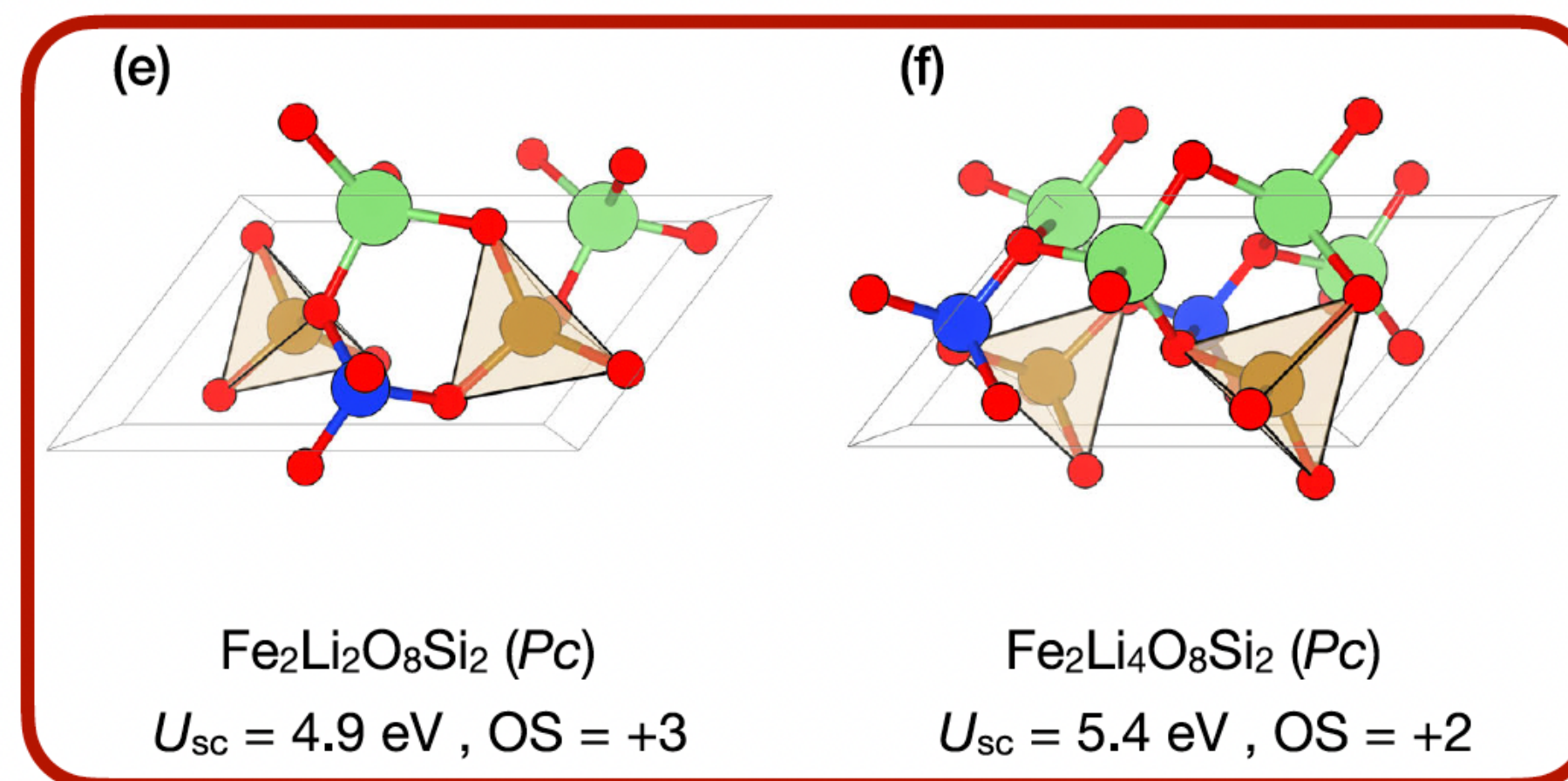
Octahedral



Square planar



Tetrahedral

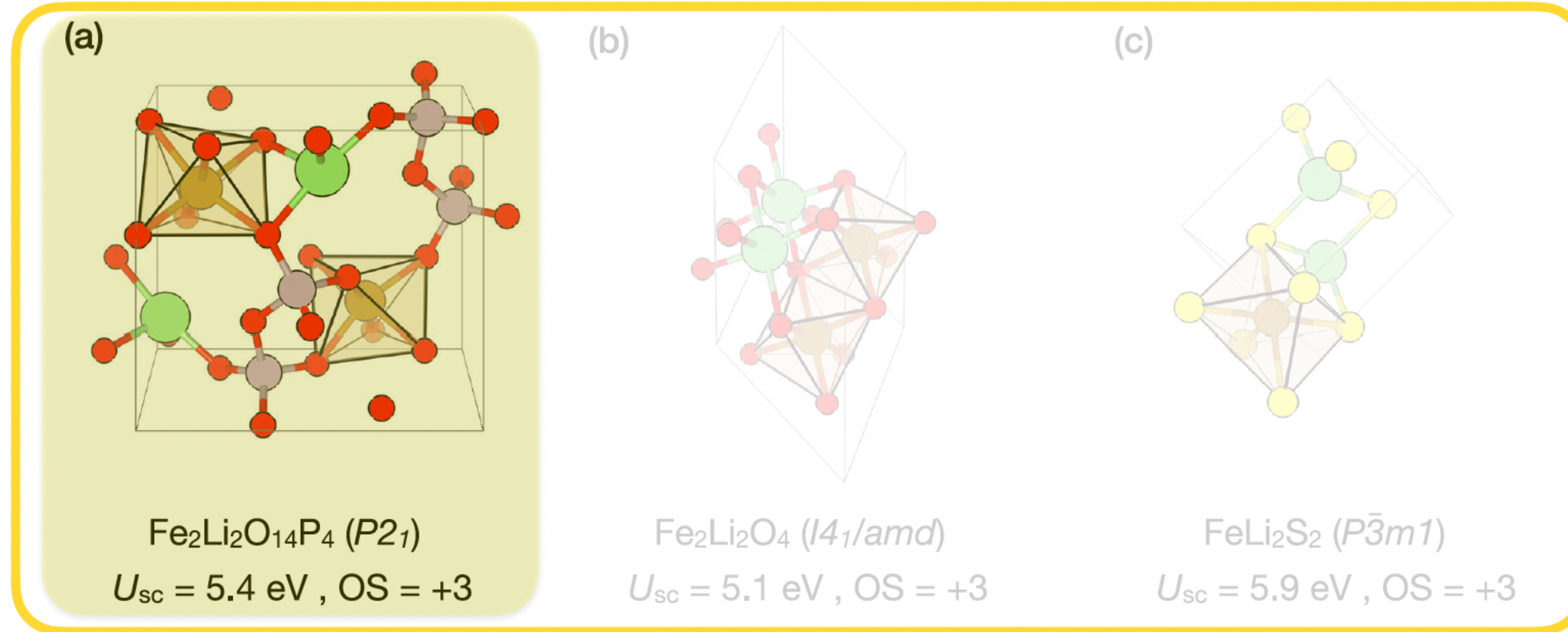


Self-consistent calculations of
Hubbard parameters for
115 Li-containing materials using
the AiiDA-Hubbard workflow

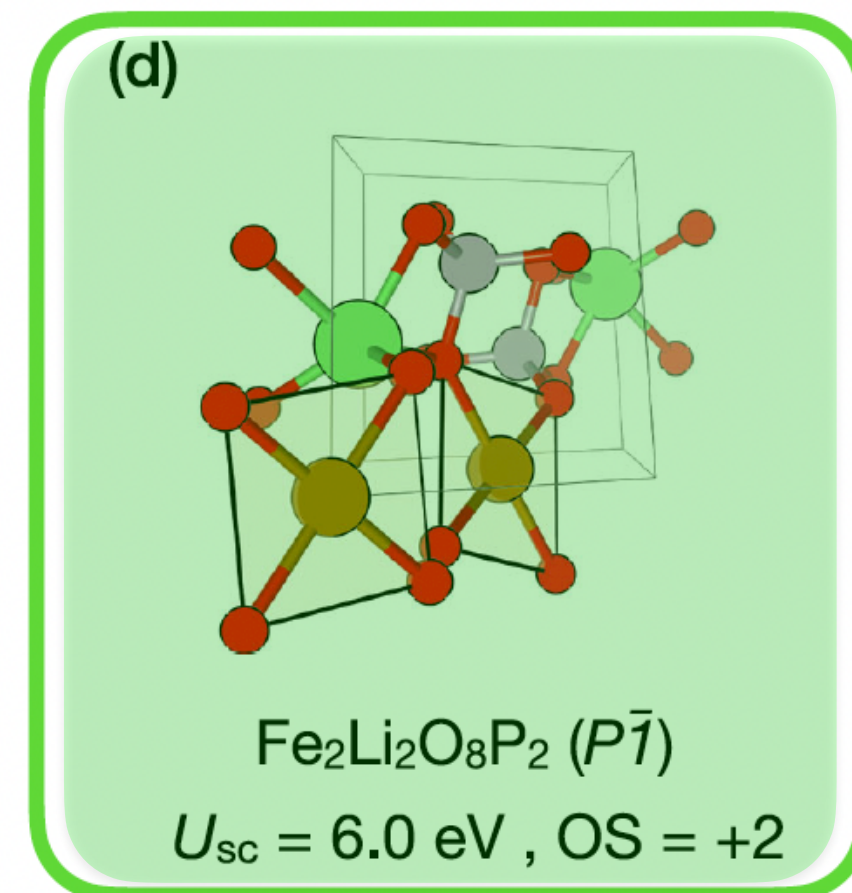


Hubbard parameters depend on many factors

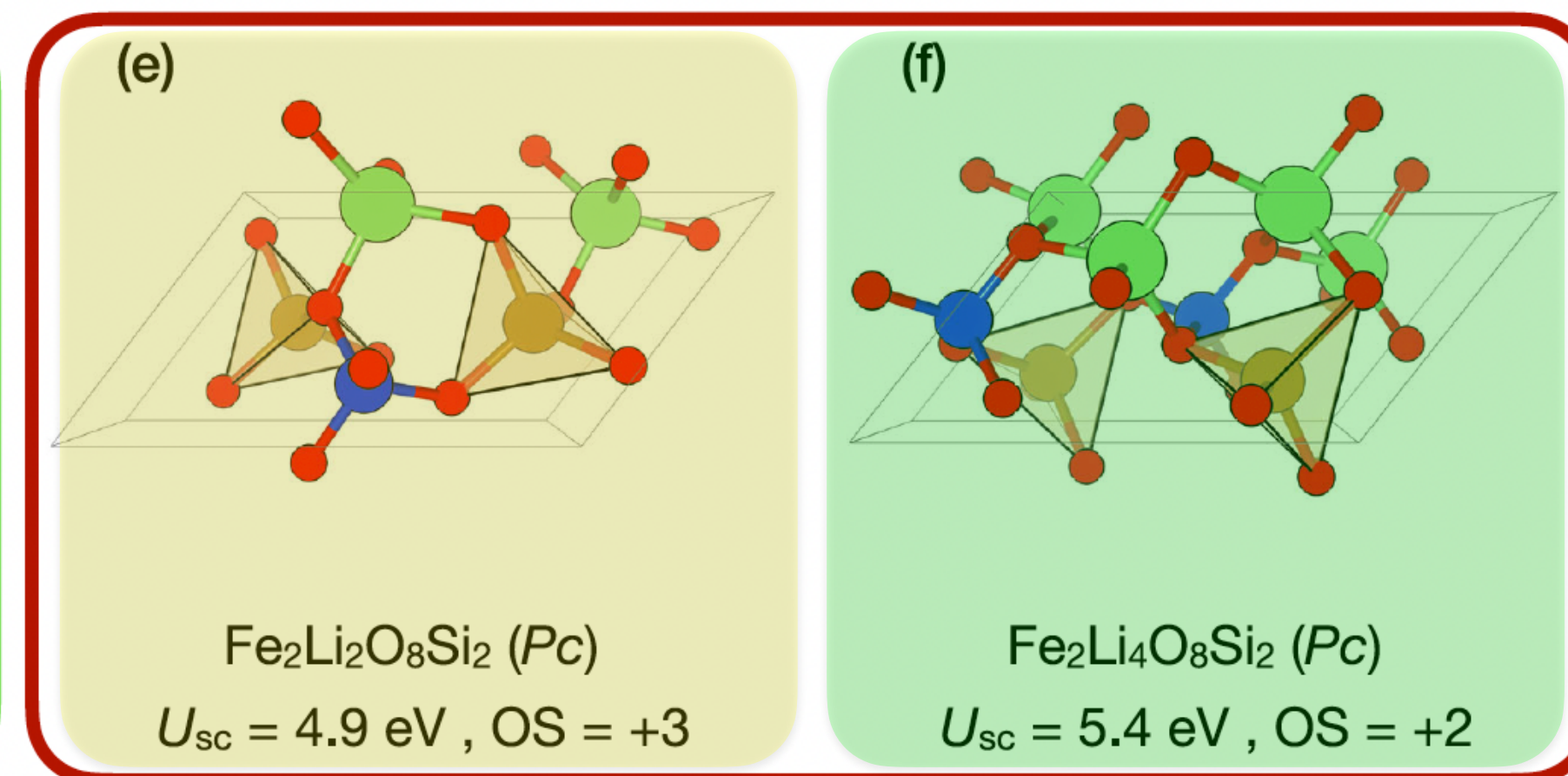
Octahedral



Square planar



Tetrahedral



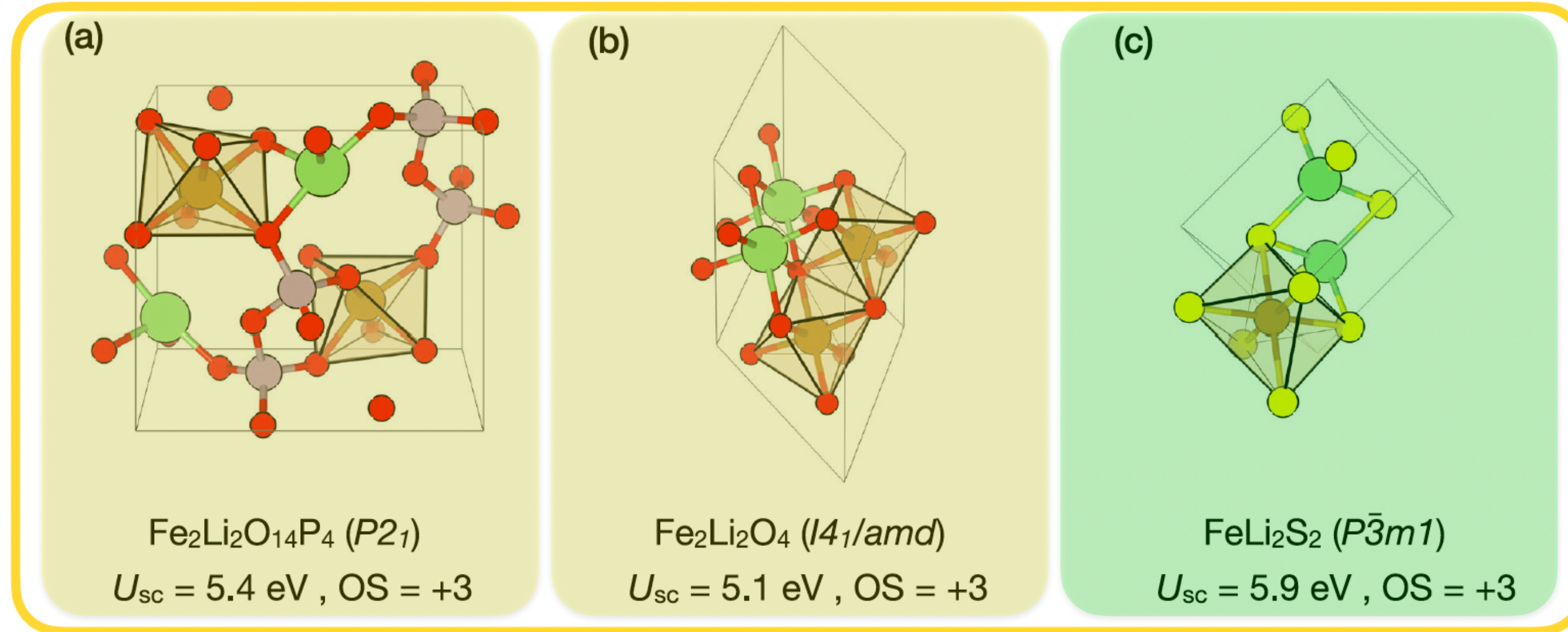
1. U dependence on coordination geometry

- Fe pairs (a,e) and (d,f):
 - Same oxidation state
 - Same oxygen ligand field (O)
 - Different coordination geometries

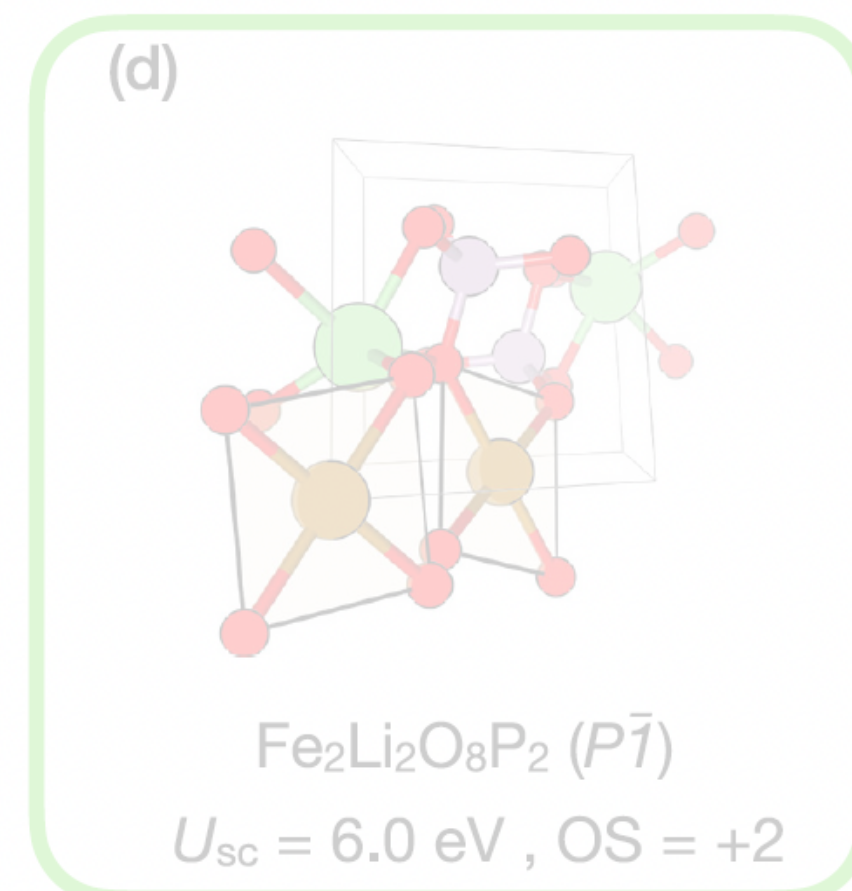
$$\Delta U \approx 0.5 - 0.6 \text{ eV}$$

Hubbard parameters depend on many factors

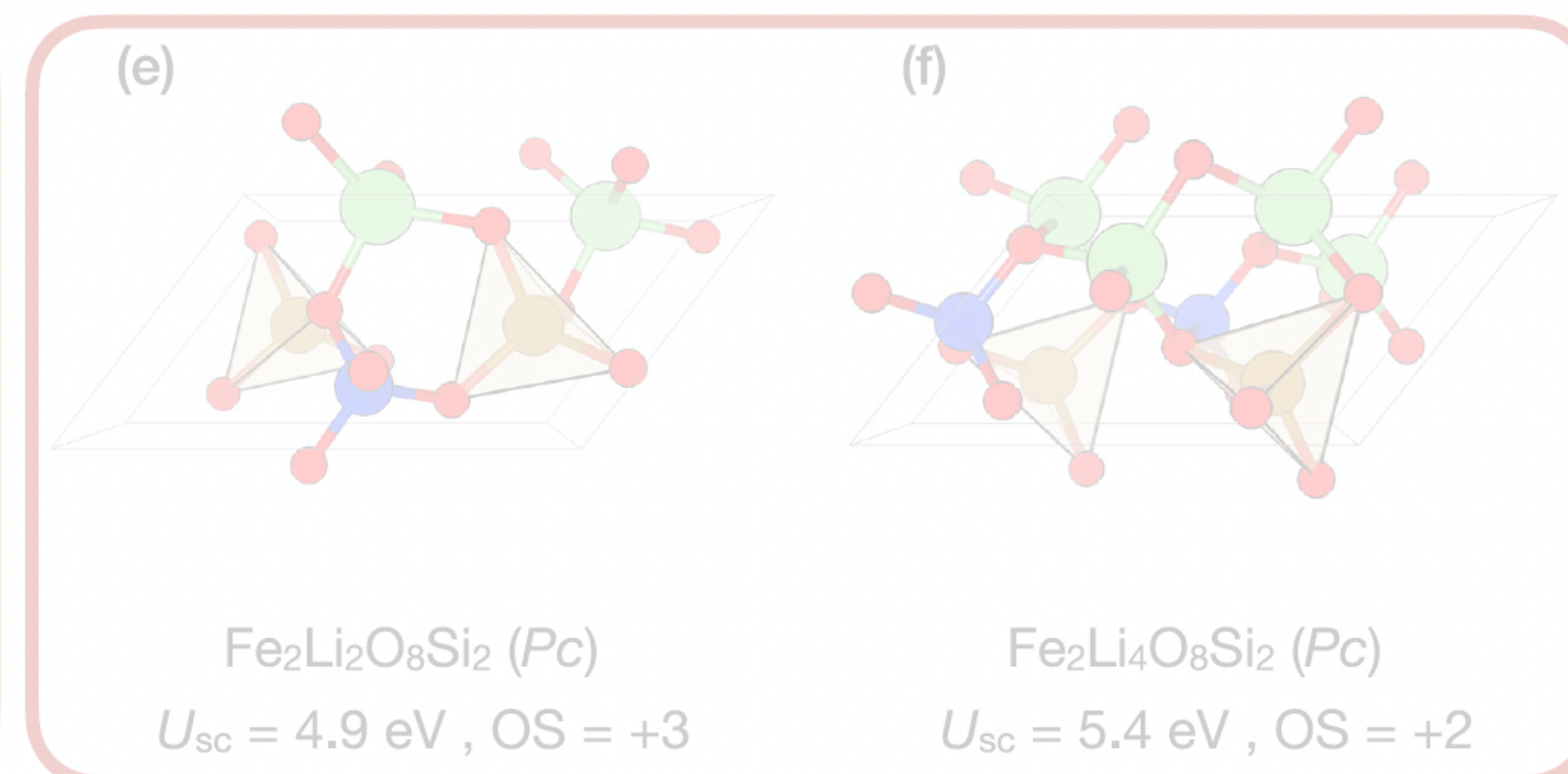
Octahedral



Square planar



Tetrahedral



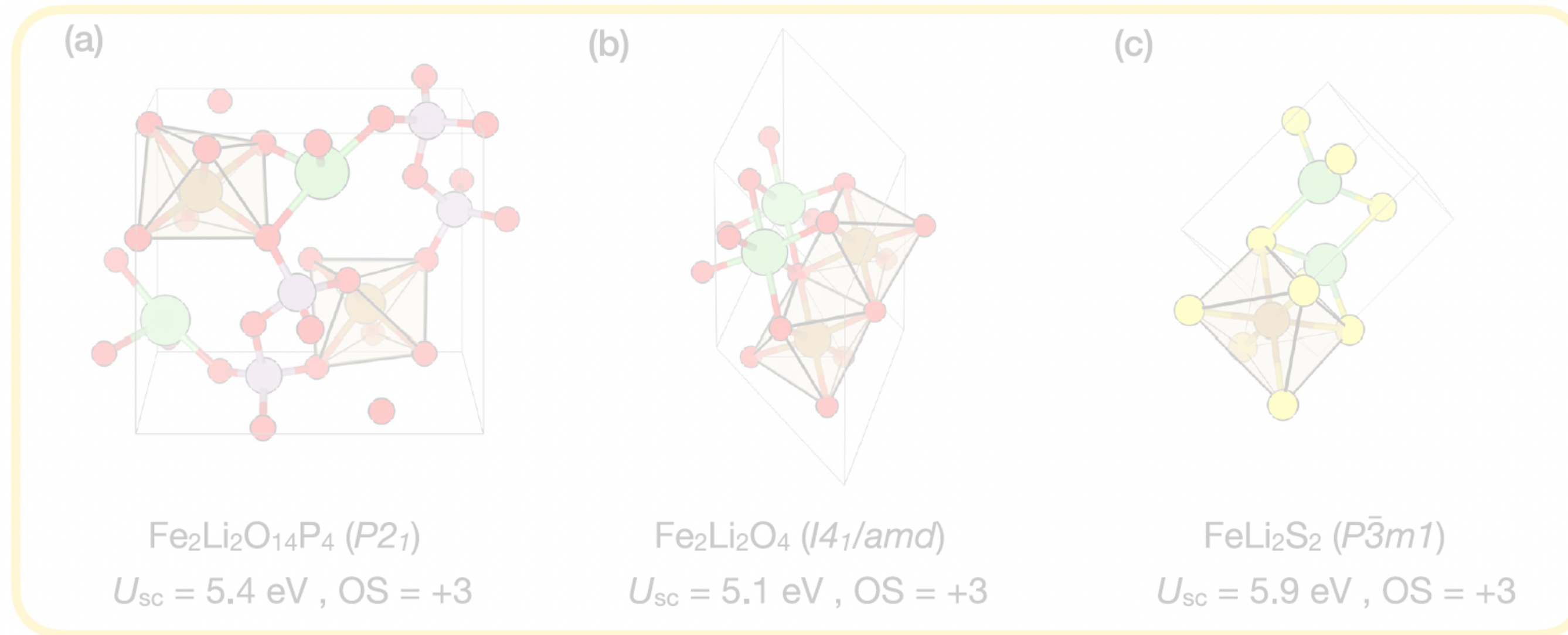
2. U dependence on ligand species

- Fe sites (a,b) vs (c):
 - Same oxidation state
 - Same octahedral coordination
 - Different ligands (O vs S)

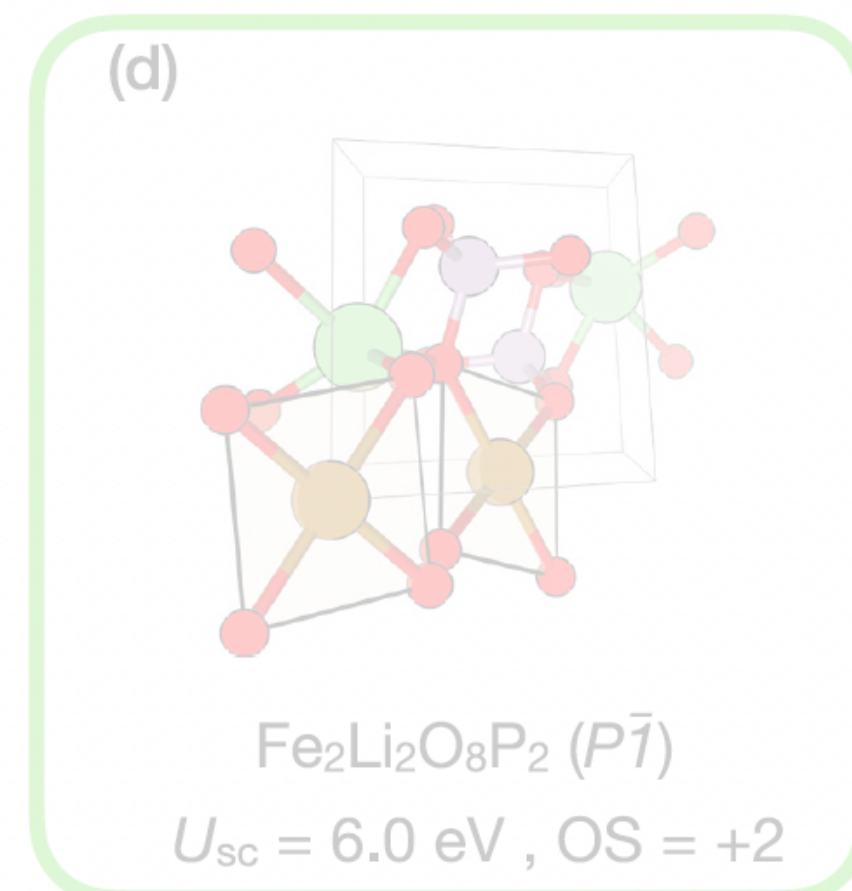
$$\Delta U \approx 0.5 - 0.8 \text{ eV}$$

Hubbard parameters depend on many factors

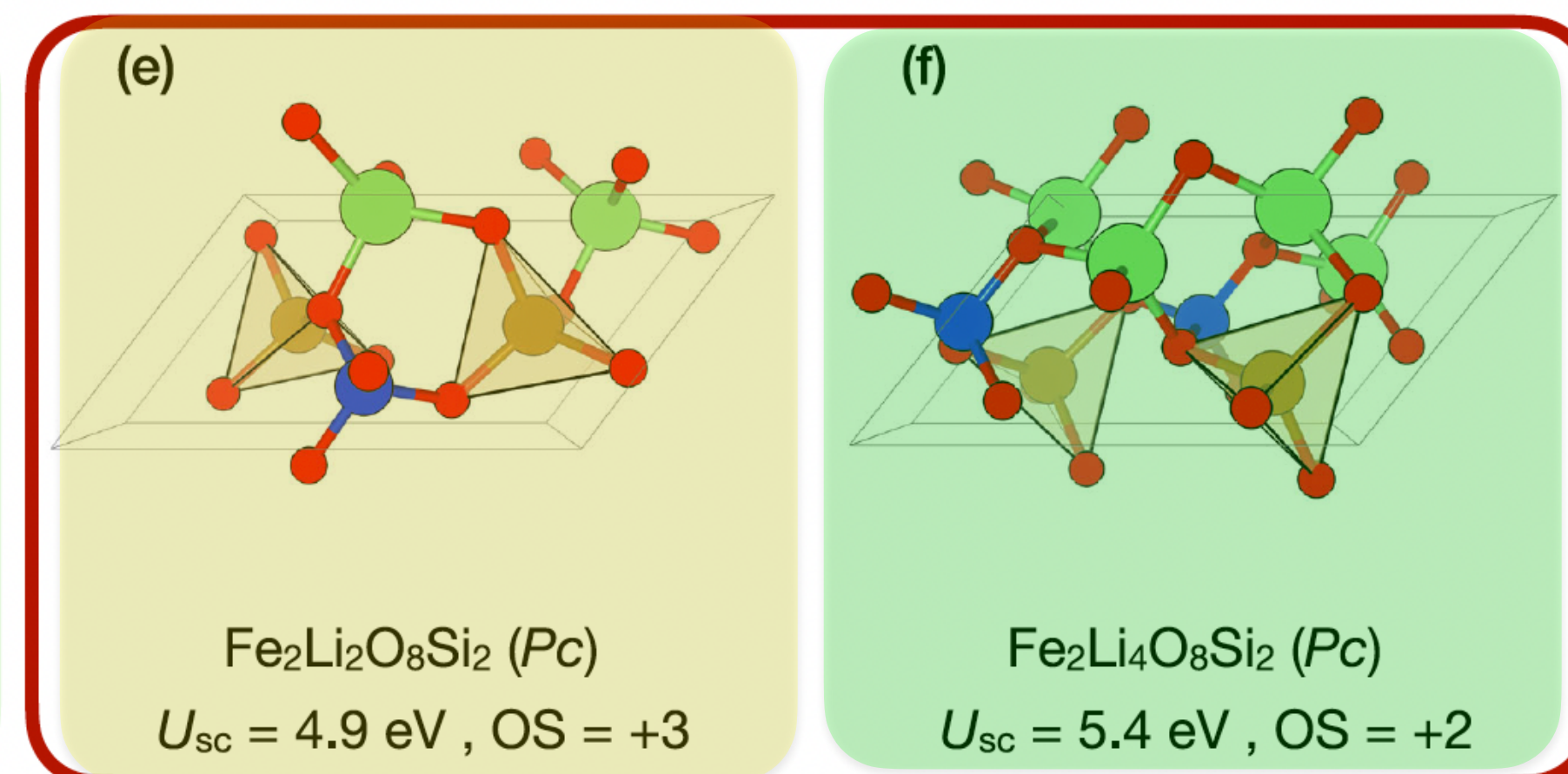
Octahedral



Square planar



Tetrahedral



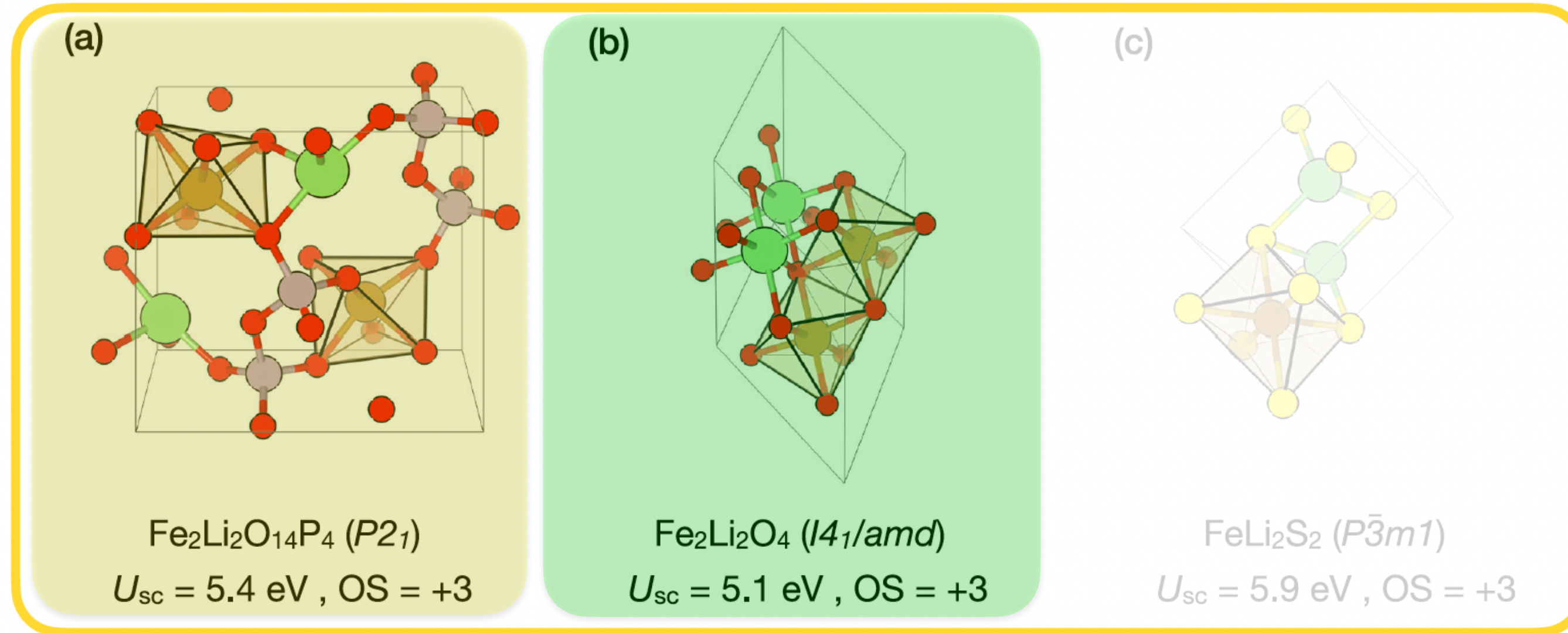
3. U dependence on oxidation state

- Fe sites (e) vs (f):
 - Same tetrahedral coordination
 - Same oxygen ligand field (O)
 - Different oxidation state (due to different amount of Li)

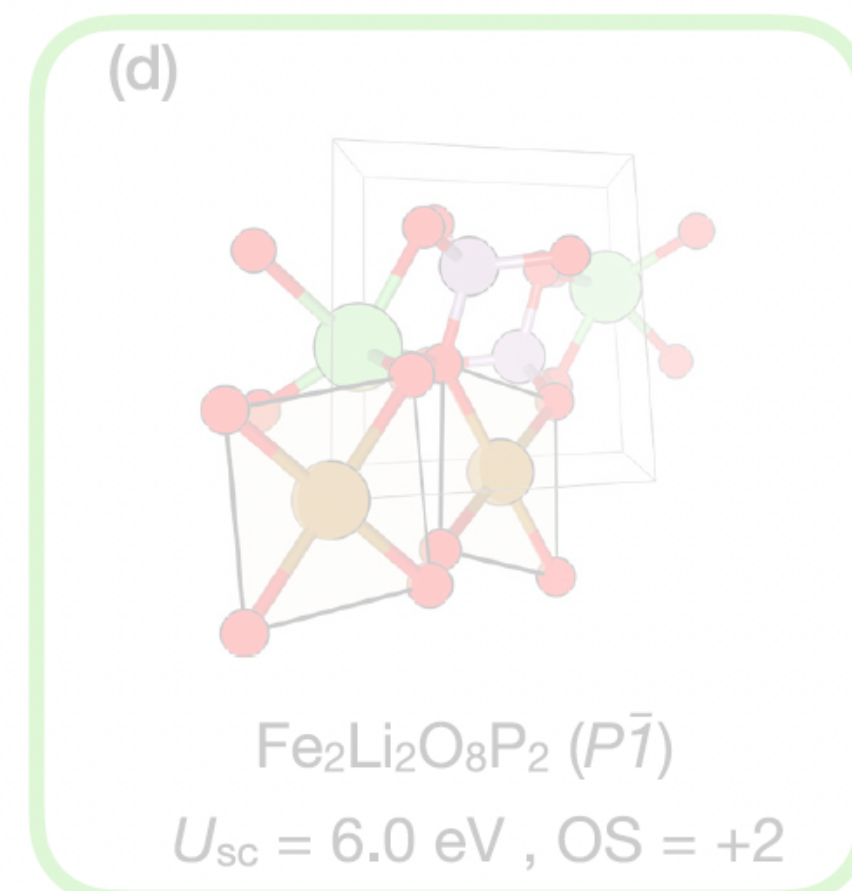
$$\Delta U \approx 0.5 \text{ eV}$$

Hubbard parameters depend on many factors

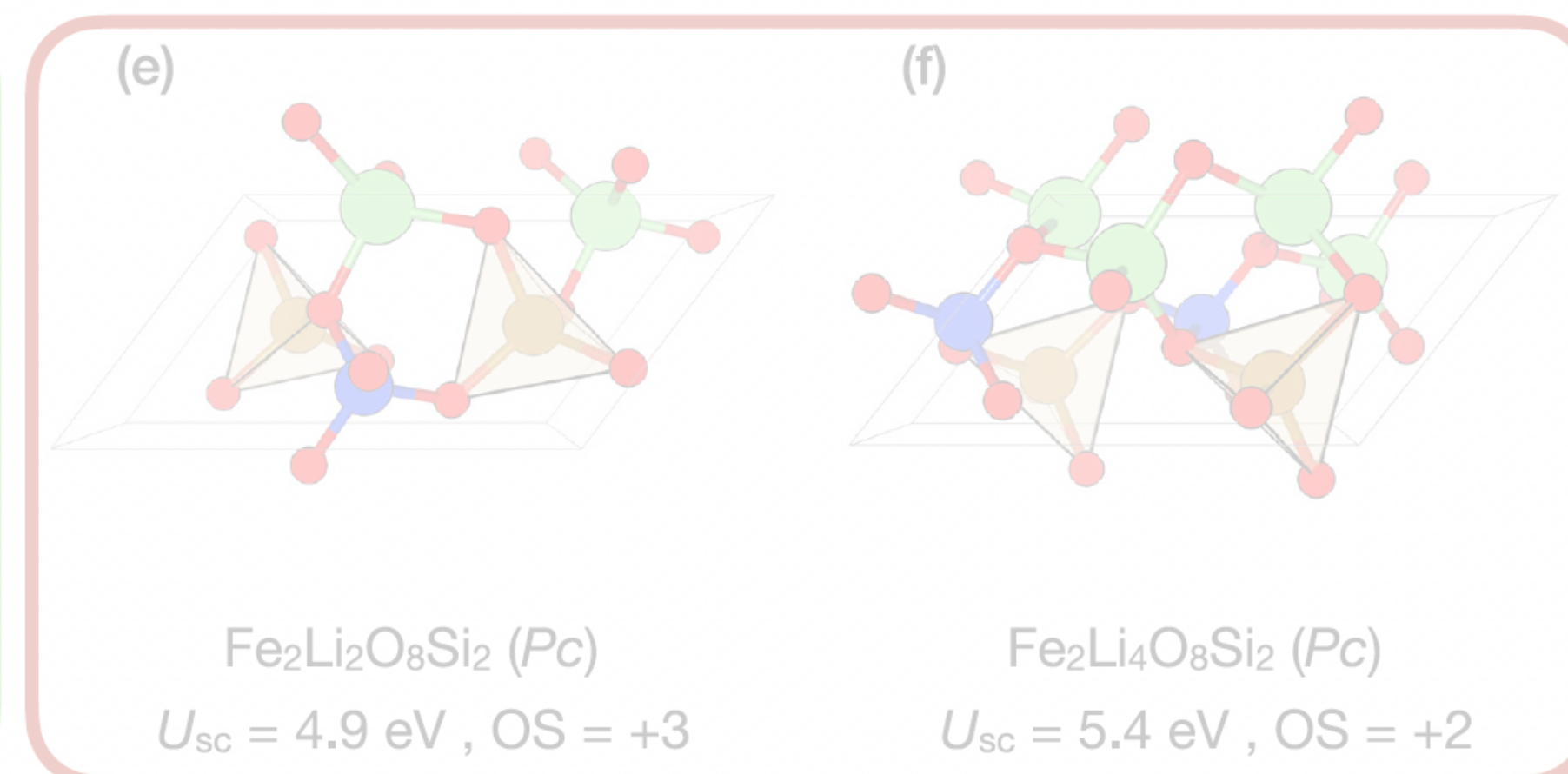
Octahedral



Square planar



Tetrahedral



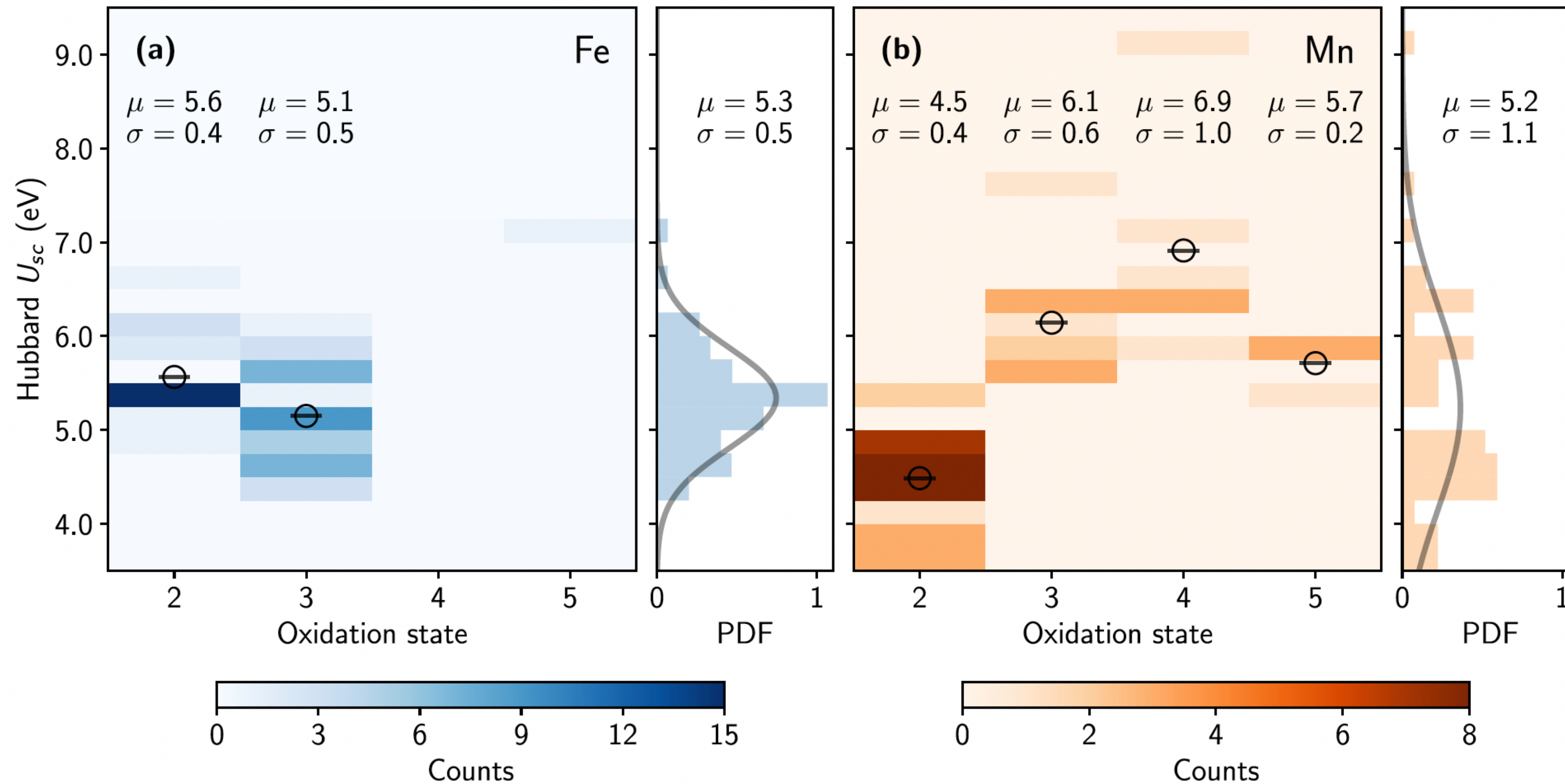
4. U dependence on local distortions

- Fe sites (a) vs (b):
 - Same octahedral coordination
 - Same oxygen ligand field (O)
 - Same oxidation state

$$\Delta U \approx 0.3 \text{ eV}$$

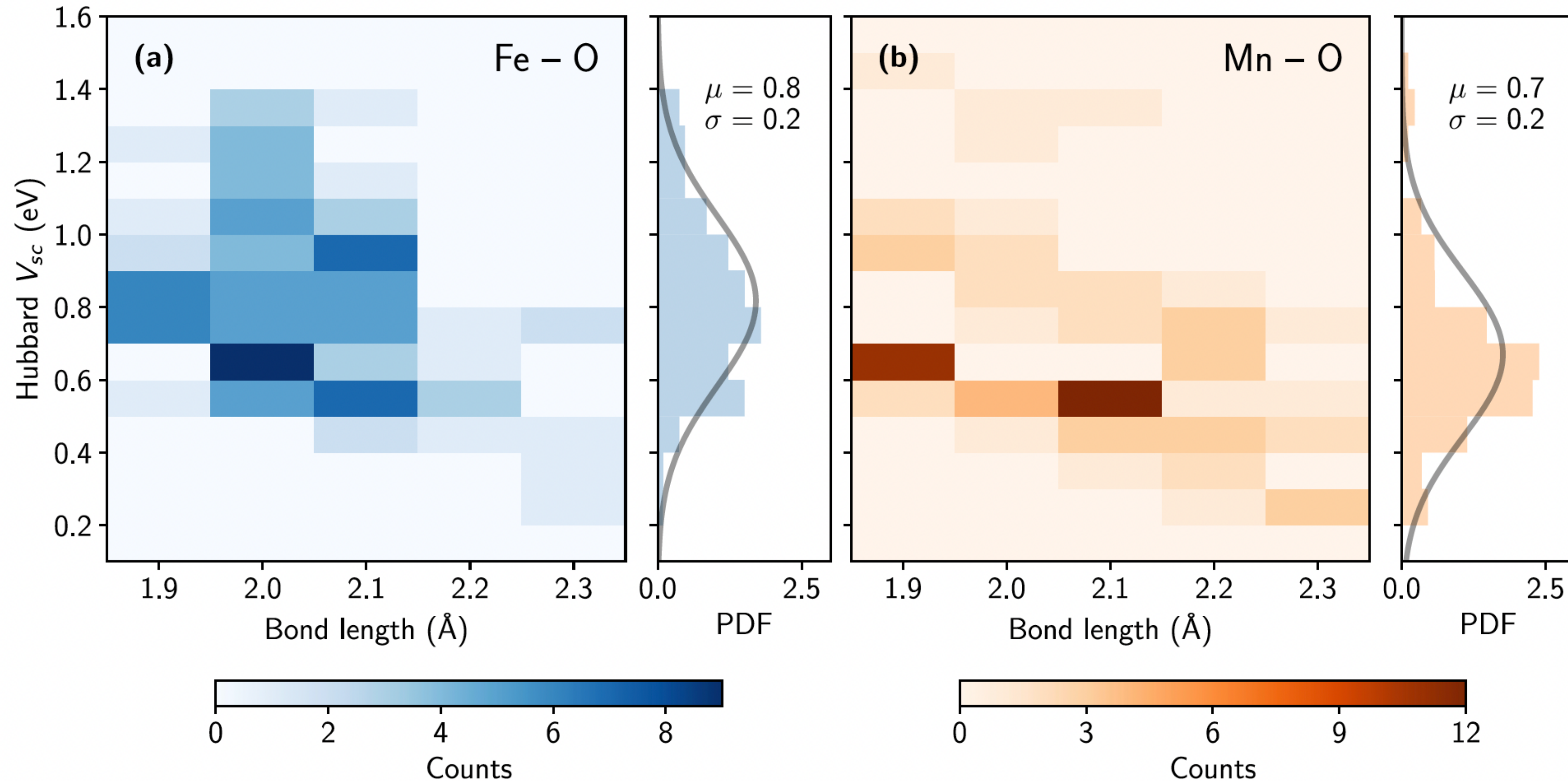
(due to changes in electronic screening)

Distribution of Hubbard U for Fe(3d) and Mn(3d)



Hubbard U is not a universal (global) parameter! It depends on many factors (OS, coordination, ligands, etc.)

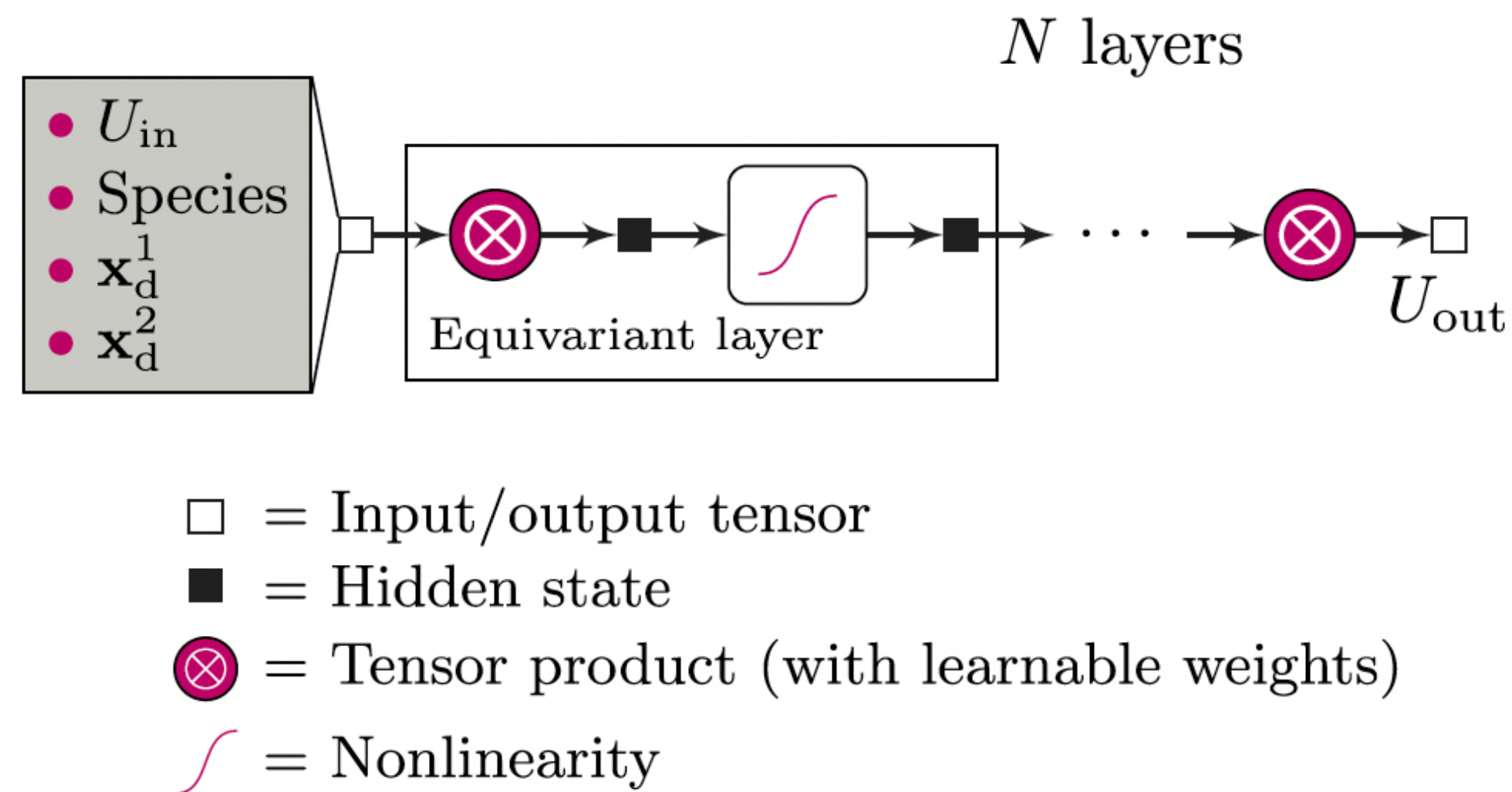
Distribution of Hubbard V for Fe/Mn-ligand



The inter-site Hubbard V decreases as the interatomic distance increases

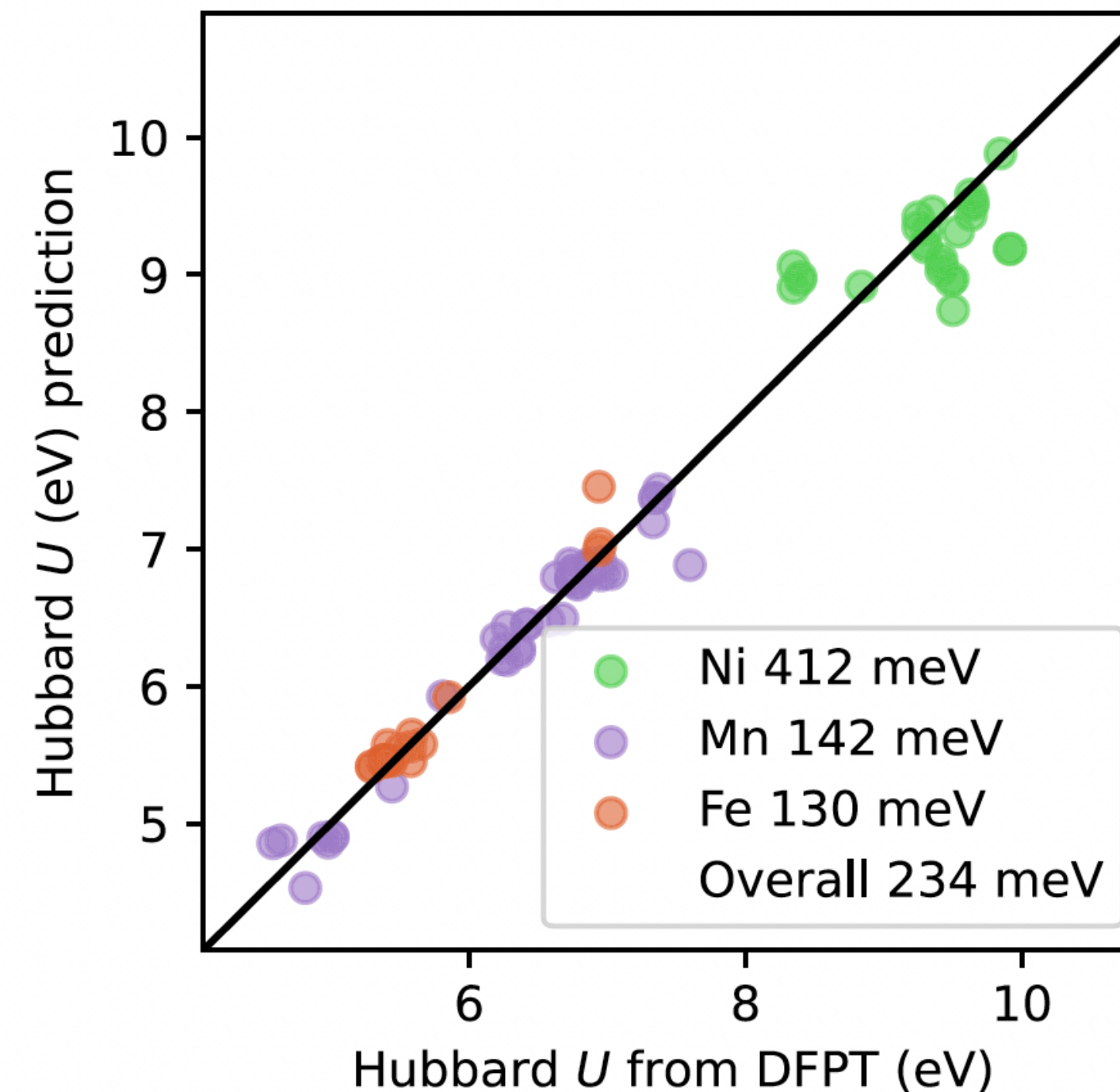
Machine learning Hubbard parameters

Equivariant neural network



On-site Hubbard U model

ML Hubbard U



Using the DFT+ U occupation matrix as the main descriptor of the ML model and DFPT U values as the training data, we machine-learn Hubbard parameters to accelerate Li-ion battery research

Take-home messages

- DFT+ U and DFT+ $U+V$ are accurate and computationally efficient approaches to model transition-metal and rare-earth compounds
- Hubbard parameters are not universal
- Hubbard parameters can be computed from first-principles using [linear-response theory](#)
- [Linear response without supercells](#): DFPT comes to the rescue
- Hubbard parameters depend on [Hubbard projectors](#)